Light-dependent orientation responses in animals can be explained by a model of compass cue integration

Kenneth Kragh Jensen

▶ **To cite this version:**

Kenneth Kragh Jensen. Light-dependent orientation responses in animals can be explained by a model of compass cue integration. Journal of Theoretical Biology, 2009, 262 (1), pp.129. 10.1016/j.jtbi.2009.09.005 . hal-00554644

HAL Id: hal-00554644
https://hal.science/hal-00554644

Submitted on 11 Jan 2011

HAL is a multi-disciplinary open access archive for the deposit and dissemination of scientific research documents, whether they are published or not. The documents may come from teaching and research institutions in France or abroad, or from public or private research centers.

L'archive ouverte pluridisciplinaire **HAL**, est destinée au dépôt et à la diffusion de documents scientifiques de niveau recherche, publiés ou non, émanant des établissements d'enseignement et de recherche français ou étrangers, des laboratoires publics ou privés.

Author's Accepted Manuscript

www.elsevier.com/locate/yjtbi

Light-dependent orientation responses in animals can be explained by a model of compass cue integration

Kenneth Kragh Jensen

PII: S0022-5193(09)00425-1
DOI: doi:10.1016/j.jtbi.2009.09.005
Reference: YJTBI5696

To appear in: *Journal of Theoretical Biology*

Received date: 7 February 2008
Revised date: 2 September 2009
Accepted date: 8 September 2009

Cite this article as: Kenneth Kragh Jensen, Light-dependent orientation responses in animals can be explained by a model of compass cue integration, *Journal of Theoretical Biology*, doi:10.1016/j.jtbi.2009.09.005

This is a PDF file of an unedited manuscript that has been accepted for publication. As a service to our customers we are providing this early version of the manuscript. The manuscript will undergo copyediting, typesetting, and review of the resulting galley proof before it is published in its final citable form. Please note that during the production process errors may be discovered which could affect the content, and all legal disclaimers that apply to the journal pertain.

ACCEPTED MANUSCRIPT

Light-dependent orientation responses in animals can be explained by a model of compass cue integration

Kenneth Kragh Jensen

Institute of Biology, University of Southern Denmark, DK-5230 Odense M, Denmark.

E-mail: kkj@jensenkk.net

Phone: 1-812-855-8709

Fax: 1-812-855-4436

Present address: Indiana University, School of Medicine, Jordan Hall, 1001 East Third Street, Bloomington, IN 47405, USA

Accepted manuscript

ACCEPTED MANUSCRIPT

Abstract

The magnetic compass sense of animals is currently thought to be based on light-dependent processes like the proposed radical pair mechanism. In accordance, many animals show orientation responses that depend on light. However, the orientation responses depend on the wavelength and irradiance of monochromatic light in rather complex ways that cannot be explained directly by the radical pair mechanism. Here, a radically different model is presented that can explain a vast majority of the complex observed light-dependent responses. The model put forward an integration process consisting of simple lateral inhibition between a normal functioning, light-*independent* magnetic compass (e.g. magnetite based) and a vision based skylight color gradient compass that misperceives compass cues in monochromatic light. Integration of the misperceived color compass cue and the normal magnetic compass not only explains most of the categorically different light-dependent orientation responses and their sequential occurrence, but also shows a surprisingly good fit to how well the animals are oriented (r-values) under light of different wavelength and irradiance. The model parsimoniously suggests the existence of a single magnetic compass in birds (probably based on magnetite) and explains the light-dependency as simple interference with another, vision based compass.

Keywords: magnetoreception; monochromatic light; light-dependent orientation responses; radical pair mechanism; magnetite.

Accepted manuscript

ACCEPTED MANUSCRIPT

Introduction

Many animals use a number of different compass cues to orient during migration. It has long been known that several animals can sense the Earth magnetic field and use it for orientation (Wiltschko and Wiltschko, 1995a). However, after more than 30 years of research it is still largely a puzzle exactly how the magnetic sense works and where the sense organ is located. Two major competing hypotheses exist today on a sensory transduction mechanism: one is based on small iron based magnetic crystals (IBMC) like magnetite and the other a chemical compass based on magnetic properties of radical pairs excited by light called the radical pair mechanism (see reviews in e.g. Johnsen and Lohmann, 2005; Johnsen and Lohmann, 2008; Wiltschko and Wiltschko, 2005).

The transduction mechanism based on IBMC is generally hypothesized to consist of the interaction of the Earth magnetic field with the magnetic crystals which then induce stress and strain on associated membranes with mechanosensitive ion channels (see e.g. Johnsen and Lohmann, 2005; Johnsen and Lohmann, 2008; Solov'yov and Greiner, 2008; Walker, 2008). In vertebrates, there is good support of the existence of such an IBMC compass system in the nasal region of rainbow trout (*Oncorhynchus mykiss*) (Diebel et al., 2000; Walker et al., 1997) and in the skin of the upper beak and nasal region of a number of birds (Beason and Nichols, 1984; Fleissner et al., 2007; Fleissner et al., 2003; Hanzlik et al., 2000; Williams and Wild, 2001; Winklhofer et al., 2001). Several theoretical considerations support that IBMC can function as a magneto reception system with no major problems (Davila et al., 2003; Davila et al., 2005; Edmonds, 1992; Fleissner et al.,

Accepted manuscript

ACCEPTED MANUSCRIPT

2007; Kirschvink and Gould, 1981; Kirschvink and Walker, 1985; Shcherbakov and Winklhofer, 1999; Solov'yov and Greiner, 2007; Solov'yov and Greiner, 2008; Walker, 2008; Winklhofer et al., 2001; Yorke, 1979; Yorke, 1981; Yorke et al., 1985).

The radical pair mechanism is hypothesized to consist of light induced radical pairs that due to their spin configuration obtain magnetic moments. The recombination of the radical pairs may then be affected by the orientation of the molecules relative to the Earth magnetic field (Ritz et al., 2000; Schulten, 1982; Schulten et al., 1986). Currently, the major candidate molecules are the cryptochromes which are known to serve functions mainly in circadian rhythms (Ritz et al., 2000; Sancar, 1999; Sancar, 2003). Many conditions must be met if such a reaction is going to be sensitive to the weak Earth magnetic field, but it may not be impossible and theoretical considerations support the principles of the radical pair mechanism as a basis for magnetoreception (Adair, 1999; Cintolesi et al., 2003; Efimova and Hore, 2008; Maeda et al., 2008; Rodgers and Hore, 2009; Solov'yov and Schulten, 2009; Solov'yov et al., 2007; Wang et al., 2006; Weaver et al., 2000).

The intriguing fact that the orientation response of many animals is indeed dependent on light has so far been taken as major support of the radical pair mechanism (for reviews see e.g. Johnsen and Lohmann, 2008; Wiltschko and Wiltschko, 2006; Wiltschko and Wiltschko, 2002). However, the observed light-dependency of orientation responses is rather complex and the experiments have left us with quite a puzzle to explain: depending on the wavelength and irradiance of monochromatic light the animals may orient in the normal expected direction, shift their orientation by 90˚relative to that direction, orient towards some unexplainable fixed direction, or be completely disoriented in spite of

Accepted manuscript

ACCEPTED MANUSCRIPT

being perfectly able to see (Johnsen et al., 2007; Wiltschko and Wiltschko, 2006). Such complex responses do not follow directly from the radical pair mechanism. Furthermore, there are cases of both normal and shifted orientation responses at longer wavelengths (Muheim et al., 2002b; Wiltschko et al., 2004b) where cryptochromes have limited to no absorption (Johnsen et al., 2007) and there are cases of disorientation at wavelengths well within the cryptochrome's absorption spectrum (Wiltschko et al., 2007a; Wiltschko et al., 2003). Therefore, there might be an alternative explanation to the light-dependency.

In addition to a magnetic compass many animals use celestial compass cues like the stars, the position of the sun, skylight polarization patterns and color gradients (Wiltschko and Wiltschko, 1999a). Obviously, a celestial compass involves vision and light. If such a sensory system is based on a system of photoreceptors that have different spectral sensitivities it may result in unexpected outputs in the highly unnatural stimulus of monochromatic light stimulates only subsets of the photoreceptors.

Multiple compass cues show clear evidence of being integrated into a single general system and specific compass mechanisms are thought not to be entirely independent from others (Wiltschko et al., 1994). Here, a model is proposed that provides a very different alternative explanation of the light-dependent orientation responses in animals. The model is cue integration based on simple lateral inhibition between "compass neurons" in compasses of different sensory modes: a color gradient compass and a magnetic compass. The integration is proposed to normally serve to increase the reliability and precision of an overall compass (Wiltschko et al., 1994). With propositions on how a color gradient sensory system may work, the model can explain a great deal of the observed complex pattern of light dependent orientation responses. In addition, the model predicts,

Accepted manuscript

ACCEPTED MANUSCRIPT

surprisingly well, the concentration of the orientation responses (r-values) as a function of light wavelength or irradiance. Contrary to the current view of a dual magneto sensory system (IBMC and radical pair) the model parsimoniously suggests that animals have only a single magnetic field sensory system (most likely is based on IBMC) and gives the simplest explanation yet of the complex patterns of light-dependent orientation responses in animals.

Methods

First, simplified models of a magnetic and a color gradient compass will be proposed. Then an integration process between two such compasses will be put forward. Propositions will then be made on how such a color gradient compass might lead to misperceptions in monochromatic light of different wavelengths and irradiances. Finally, it will be demonstrated how the integration model behaves in monochromatic light when such an abnormal output of the color gradient compass is integrated with the normal output from an intact magnetic compass.

A magnetic compass

An orientation cue is some geophysical or celestial parameter that can be used for discriminating geographical directions. Let's begin by assuming a strongly simplified hypothetical magnetic compass sensory system consisting of a circular array of compass cells with the axis of each cell body pointing in a different geographical direction (Fig. 1A) (as proposed by Deutschlander et al., 1999; Phillips and Borland, 1992a). A specific transduction mechanism is not essential to the model and several suggestions can be found elsewhere (see introduction for references). So let us just assume without any detail of a

Accepted manuscript

ACCEPTED MANUSCRIPT

transduction mechanism that the compass cells with their cell axis aligned parallel to the magnetic field lines along the magnetic North-South axis are maximally excited, resulting in maximal neural spike frequencies. Oppositely, the cells having their axes aligned along the East-West axis, perpendicular to the magnetic field, are minimally excited and fire with some spontaneous spike frequency. Thus there will be a non-uniform circular distribution of spike frequencies among the cells along all 360˚ that has its maximum along the magnetic North-South axis and minimum along the East-West axis. A simple non-uniform circular distribution is the elliptic form. Let us therefore assume that the spike frequencies, *SF*, as a function of geographical direction, ω, follow a simple elliptic form and can be represented mathematically by a standard ellipse equation as:

$$SF(\omega)_{mag} \approx \frac{A_{mag} \cdot B_{mag}}{\sqrt{A_{mag}^2 \cdot \cos^2(\omega) + B_{mag}^2 \cdot \sin^2(\omega)}} \qquad \text{(Equation 1)}$$

where the constants A_{mag} and B_{mag} represents the average spike frequency along the maximal excited and the minimal excited axis respectively corresponding to the major and minor axis of an ellipse. In the following the major and minor axes *A* and *B* will be referred to as the *major* and *minor compass axis,* respectively. $SF(\omega)_{mag}$ can then be represented as radial values in a polar plot as shown innermost in Fig. 1A with the radius in any given direction corresponding to the average spike frequency of the cells with their axis pointed in that direction. Larger radial values correspond to higher spike frequencies. The spike

Accepted manuscript

ACCEPTED MANUSCRIPT

153 frequency in any given direction will be referred to as the *radial spike frequency*. The
154 circular distribution of spike frequencies will be referred to as the *directional firing pattern*.

155 **A color gradient compass**

156 The position of the sun is an important cue used by many animals for orientation
157 (see e.g. Wiltschko and Wiltschko, 1993). Scattering of the sunlight in the atmosphere
158 results in polarization patterns, intensity, and color gradients that are all dependent on the
159 position of the sun and can be used to reveal its position when it is not directly visible. The
160 color gradients consist of an increased amount of long wavelength light relative to short
161 wavelength/UV light in the direction of the sun and, oppositely, an increased amount of
162 short wavelength/UV light relative to longer wavelengths in the anti-solar direction,
163 whereas there is a more balanced distribution at an angle of 90° relative to the direction of
164 the sun (Fig. 1B) (Coemans et al., 1994). Although it is known that key navigators like bees
165 and ants are able to use color gradients for rather precise orientation (Rossel and Wehner,
166 1984; Wehner, 1997), there has been surprisingly little focus on animal orientation by color
167 gradients . Given the simplicity and apparent efficiency of color cues, it is thus not unlikely
168 that color gradients are used by a wide number of animals for orientation including the
169 passerine birds. A model color gradient compass may be based on a simple contrast
170 between UV and long wavelength light:

171

172 $$SF(\omega)_{col} \approx |SF_{UV}(\omega) - SF_{LW}(\omega)| \approx \frac{A_{col} \cdot B_{col}}{\sqrt{A_{col}^2 \cdot \cos^2(\omega) + B_{col}^2 \cdot \sin^2(\omega)}}$$ (Equation 2)

173

Accepted manuscript

ACCEPTED MANUSCRIPT

$SF(\omega)_{col}$, in any given direction, is the absolute difference between the spike frequency elicited by a UV photoreceptor mechanism, $SF_{UV}(\omega)$, and that of a long wavelength sensitive photoreceptor mechanism $SF_{LW}(\omega)$. $SF(\omega)_{col}$ would then be maximal (A_{col}) along the solar-anti solar axis (solar meridian) where the spectral contrast is maximal and minimal along the axis 90° relative to the solar meridian where the contrast is minimal (B_{col}). Therefore, as for the magnetic compass, we will assume that there exists a circular array of color gradient compass cells which will show a simple elliptic form of the directional firing pattern (see Fig. 1B).

It has been suggested that light in the blue or mid wavelength range may serve as some sort of reference color in a color gradient compass (Kinoshita et al., 2007). In that case Eq. 2, which will be returned to later, becomes:

$$SF(\omega)_{col} \approx \frac{|SF_{UV}(\omega) - SF_{LW}(\omega)|}{SF_{SW-MW}(\omega)} \qquad \text{(Equation 3)}$$

where $SF_{SW\text{-}MW}$ is the spike frequencies elicited by a photoreceptor mechanism in the short and/or mid wavelength range. A high input from the SW – MW range relative to both the UV and the LW range would then tend to inhibit the color compass spike frequency.

Model compass integration

Animals have a multitude of compasses based on the different celestial and geophysical cues and it is thought that these multiple compasses are closely integrated into an overall compass (Able, 1991; Wiltschko et al., 1994). Lateral inhibition, where

Accepted manuscript

ACCEPTED MANUSCRIPT

neighboring neurons have a mutual inhibitory effect, is common in many sensory systems like for instance in vision contrast enhancement (Golden, 1996). Lateral inhibition is likely to occur in compass sensory systems too and could for instance function as a contrasting effect between cues ensuring that the most prominent compass cue in any given direction dominates. The current model will therefore assume that compass cues are integrated through lateral inhibition and the resultant integrated compass is assumed to be simply the absolute value of the difference in spike frequency of the two above compasses as a function of direction as shown in the following equation:

$$SF(\omega)_{int} = |SF(\omega)_{col} - SF(\omega)_{mag}| \qquad \text{(Equation 4)}$$

Let us assume that the color gradient compass has an arbitrary major compass axis of 100 spikes/s along the geographical North-South axis, $A_{col} = 100$, and let us say that the minor compass axis, the spontaneous spike frequency, is approximately one third of this, 35 spikes/s, along the East-West axis ($B_{col} = 35$). Let us assume the hypothetical magnetic compass has the same spontaneous spike frequency of 35 spikes/s along the East-West axis ($B_{mag} = 35$) but because celestial cues appear to be dominant and preferred over magnetic cues (Mouritsen, 1998; Muheim, 2006; Wiltschko et al., 1994) the precision of the magnetic compass is assumed lower and the maximal spike frequency along the North-South axis will be assigned to be, for instance, 70% of the celestial compass ($A_{mag} = 70$). Fig. 2A then shows the result of the integration (solid line; Eq. 4) of the color gradient compass (dashed line) and the magnetic compass (dotted line). As can be seen, the result of

Accepted manuscript

ACCEPTED MANUSCRIPT

the integration is a compass with a higher contrast between the North-South and East-West axes. Equally important, the compass that is maximally excited will dominate in a situation where there, for instance, is a moderate mismatch between the two compasses (Fig. 2B).

For simplicity, the model does not consider time compensation for celestial rotation in the color gradient compass or declination between the color gradient compass and magnetic compass (i.e. declination = 0). The major compass axes of the two compasses will thus always be aligned and both compass cues point out the same North-South axis. The animal's normal orientation is assumed to be towards that common compass North. North may be separated from South based on inclination in the magnetic compass (Wiltschko, 1972), and for the color gradient compass, the solar direction may be separated from the anti-solar direction by its maximal content of long wavelength light under natural conditions. Finally, we will assume that the animals do not assess the cues from each compass separately in a normal orientation context and that they will uncritically orient along the axis of maximal excitation of the integrated compass only (this may be different in a calibration context).

Behavior of color gradient compass in monochromatic light

It follows from Eq. 2 that if the incoming light is monochromatic and excites predominately the UV or the LW mechanism, the radial spike frequency of the color gradient compass, $SF(\omega)_{col}$, will be high but since the light comes from all directions, the directional firing pattern will be uniform and form a circle rather than an ellipse (i.e. $A_{col} = B_{col}$; Fig. 1C). The higher the irradiance of monochromatic light exciting predominately one color detector, the larger the $|SF_{UV} - SF_{LW}|$ difference in all directions and thus the higher

Accepted manuscript

ACCEPTED MANUSCRIPT

the radial spike frequency $SF(\omega)_{col}$ (i.e. larger radius of the circular directional firing pattern). Similarly, the more the wavelength of the monochromatic light skews towards and predominately excites one color detector over the other, the larger the $|SF_{UV} - SF_{LW}|$ difference and thus the higher the radial spike frequency $SF(\omega)_{col}$. In the following treatment, the term $SF(\omega)_{col}$ will be referred to as $SF(\omega)'_{col}$ as a reminder that the directional firing pattern is uniform and forms a circle and that its radial spike frequency ("radius") depends on the irradiance and wavelength of the monochromatic light.

Behavior of integration in monochromatic light

What happens if we do the integration with the uniform directional firing pattern suggested above? Fig. 3A shows an initial case of compass integration where the monochromatic light is assumed to excite predominately one color detector but where the irradiance is low and results in a low radial spike frequency of the color gradient compass. Here there is little effect of the color gradient compass on the integrated compass and the animals will be expected to orient normally towards the North. As the irradiance of the monochromatic light increases the radial spike frequencies of the color gradient compass, $SF(\omega)'_{col}$, will increase. At one point the integrated output will have four lobes and be equally excited in both the North-South and East-West direction and the animals will be expected to be disoriented (Fig. 3B). As the light irradiance increases further the East-West axis will start to dominate and the animals will be expected to shift their orientation by 90˚ (Fig. 3C). Then, as the light irradiance is increased further the animals will keep showing shifted orientation, but as can be seen, the precision of the compass will gradually degrade

Accepted manuscript

ACCEPTED MANUSCRIPT

and the orientation will be poorer and poorer until the animals finally show disorientation again (Fig. 3D-E). An animated sequence of the integrated compass output as a function of the model color gradient compass input is shown in Supplemental Movie 1.

A similar pattern of orientation responses is to be expected if we instead keep the irradiance of the monochromatic light constant and vary the wavelength. There will be no output from the color gradient compass if, initially, the wavelength of the monochromatic light lies within a range where the input to the UV and long wavelength mechanism is balanced. However, if we then shift the wavelength of the monochromatic light towards the sensitivity of the UV or the LW receptors, then the radial frequency, $SF(\omega)'_{col}$, will increase. Therefore, the more the wavelength of the monochromatic light moves towards the spectral sensitivity of the UV or the long wavelength receptors, the more the radial spike frequencies, $SF(\omega)'_{col}$, increase and (if the irradiance is high enough) we will expect to observe the exact same sequence of orientation responses going from normal (Fig. 3A), to disoriented (Fig. 3B), to a 90˚ shift (Fig. 3C), and again towards disoriented (Fig. 3D-E).

Model predictions of a mosaic pattern of orientation responses

It has now been shown how the hypothetical integration process is influenced as a function of the relative excitation level of the color gradient compass photoreceptors. Let us now consider what categories of orientation responses the model predicts to be distributed around the spectral sensitivities of the color detectors as a function of both wavelength and intensity of the light. Let us assume that we have a color gradient compass of the type proposed above with a UV and a LW detector (Fig. 4). Let us first assume that animals in

Accepted manuscript

ACCEPTED MANUSCRIPT

281 an orientation test are placed under illumination of monochromatic light of constant
282 wavelength close to the peak spectral sensitivity of either the UV or long wavelength
283 detectors (arrows 1). Under very low irradiances the output from the color gradient
284 compass will be minimal and not affect the orientation (black "N"). As the irradiance is
285 increased the animals will show the predicted sequence of orientation responses (c.f. Fig. 3
286 and see above) going from normal orientation, to disorientation (light gray "D"), to 90˚
287 shift (darker grey "S"), and towards disorientation again. Oppositely, if the wavelength of
288 the monochromatic light lies between the peak spectral sensitivities of the UV and LW
289 detectors in a range where they are equally excited, then $SF(\omega)'_{col}$ will be constantly low
290 and the orientation will stay normal and independent of irradiance (arrow 2).
291 Let us instead keep the irradiance constant and vary the wavelength (double arrow
292 3). If the wavelength is at first kept between the UV and LW receptors (middle of arrow 3)
293 the orientation will be normal as mentioned above, but as we change the wavelength
294 towards either the UV or LW detectors then these will start being increasingly excited
295 relative to the other detector and the model predicts an identical sequence of orientation
296 responses with responses going from normal, to disoriented, to shifted, and back to
297 disoriented.
298 The further the wavelength of the monochromatic light is placed towards the
299 spectral sensitivity of the UV or LW detectors, the lower the irradiance of the
300 monochromatic light is necessary to excite that detector a certain amount relative to the
301 other detector. We will therefore expect that the further the wavelength of the
302 monochromatic light is skewed towards the spectral sensitivity of one of the detectors, the

Accepted manuscript

ACCEPTED MANUSCRIPT

lower the irradiance is necessary to elicit a given orientation response and the response sequence ($N \rightarrow D \rightarrow S \rightarrow D$) will start at lower and lower irradiances. This is illustrated by arrows 4 where, if we for instance fix the attention to the shifted orientation response (S), we will expect this particular response to occur at lower and lower irradiances as we go towards the spectral sensitivity of the UV or LW detectors. The proposed relationship between orientating responses and the absorption spectra of the detectors is highly suggestive and the exact relationship must depend on factors like the specific form of the detector's absorption spectra, the relative sensitivity of the detectors, and the overlap between the detectors.

Predictions on the concentration of orientation (r-value)

The r-value is used in circular statistics as a measure of the concentration of individual headings around the mean direction (Batschelet, 1981). An r-value of 1 indicates that the experimental animals are all headed in the exact same direction. An r-value of 0 indicates that the animals were totally disoriented and headed with equal probability towards any direction. The precision by which a group of animals head towards a common goal must strongly depend on the precision of their available compasses. It is fair to assume for our hypothetical array of compass neurons that the more excited the cells coding the North-South axis are relative to the cells coding the East-West axis, the more precise the overall compass works and the better the animals are expected to be oriented. A common measure of the relative sizes of the axes in an ellipse is the eccentricity. The eccentricity for a compass will be termed the compass eccentricity, $\varepsilon_{c,}$ and is defined as follows:

Accepted manuscript

ACCEPTED MANUSCRIPT

$$\varepsilon_c = \sqrt{1 - \frac{B_c^2}{A_c^2}} \qquad \text{(Equation 5)}$$

A_c and B_c are the major and minor compass axes of the given compass (see above). The eccentricity varies between 0 and 1 with 0 indicating a circle and 1 an extreme oval form. A compass is useless in pointing out directions and cause disorientation and r-values near 0 when the major and minor compass axes are equal $(A_c = B_c)$ and $\varepsilon_c = 0$ and will have an optimal precision and cause strong directional headings with r-values near 1 when $A_c \gg B_c$ and ε_c goes towards 1. Thus we expect r-values and compass eccentricities to be highly correlated.

Fig. 5 shows how the compass eccentricity of the integrated compass changes as a function of $SF(\omega)'_{col}$ (calculated as in Fig. 3 with $A_{mag} = 70$ and $B_{mag} = 35$ for the magnetic compass). Fig. 5 also contains references to each of the examples in Fig. 3 (A-E) where the directional firing pattern of the integrated compass can be seen for comparison. It should be noted that the directional firing pattern of the integrated compass is obviously more complex than the elliptic form and the compass eccentricity, which is defined for an ellipse, strictly does not apply. However, this treatment seems quite adequate for the current purpose and still gives a good measure of the contrast between the North-South and East-West axis of the compass.

Accepted manuscript

ACCEPTED MANUSCRIPT

Fitting compass eccentricity to observed r-values

As mentioned above the compass eccentricity, ε_c, is expected to be highly correlated with r-values and it is predicted that r-values in the literature will follow a similar pattern to that of the compass eccentricity in Fig. 5. Therefore, in the following, fits of Eq. 5 as a function of $SF(\omega)'_{col}$ will be made to r-values in the literature. However, in practice there is a problem in the fact that the compass eccentricity in Eq. 5 cannot easily be used as a fitting function in a simple mathematical way because when the integration compass shifts 90˚ as $B_{int} > A_{int}$ we end up with the square root of a negative number. To solve this, the following equation has been developed which does not have that problem and comes very close to the conventional eccentricity measure:

$$\varepsilon_c = \left|\frac{(A_{int})^2-(B_{int})^2}{(A_{int})^2+(B_{int})^2}\right|^{0.314} = \left|\frac{(A_{col}-A_{mag})^2-(B_{col}-B_{mag})^2}{(A_{col}-A_{mag})^2+(B_{col}-B_{mag})^2}\right|^{0.314} \quad \text{(Equation 6)}$$

The parameter 0.314 was found by iterative fitting of Eq. 6 to curves of Eq. 5 (see Fig. A1 in the appendix).

Scaling along both the abscissa and ordinate is necessary in order to fit the theoretical compass eccentricities to the wavelength and irradiance data ranges of the real r-values. This will be done by including some simple scaling parameters to Eq. 6. It turns out that scaling along the abscissa provides a better fit to the irradiance and wavelength scale when this is done by exponential transformation whereas it suffices with simple

Accepted manuscript

ACCEPTED MANUSCRIPT

multiplication along the ordinate. Therefore, the literature data will be fitted by the following equation:

$$s_c\left(SF(\omega)^{\circ}_{col}\right) = n \cdot \left| \frac{\left(k \cdot 10^{m \cdot SF(\omega)^{\circ}_{col}} - A_{mag}\right)^2 - \left(k \cdot 10^{m \cdot SF(\omega)^{\circ}_{col}} - B_{mag}\right)^2}{\left(k \cdot 10^{m \cdot SF(\omega)^{\circ}_{col}} - A_{mag}\right)^2 + \left(k \cdot 10^{m \cdot SF(\omega)^{\circ}_{col}} - B_{mag}\right)^2} \right|^{0.814} \quad \text{(Equation 7)}$$

The parameter n is then the linear multiplication factor for scaling along the ordinate and k and m are the parameters for exponential scaling along the abscissa. The parameters of the model magnet compass were kept constant during the fitting procedure with $A_{mag} = 70$ and $B_{mag} = 45$. These constant values of the magnetic compass seemed to give the best fits and were determined initially through fitting procedures with B_{mag} as an additional parameter. The effect of changing the various fitting parameters is shown in Fig. A2 of the appendix.

As an indication of the goodness of fit the adjusted correlation coefficient R_{adj} is reported in the results. R_{adj} compensates for the number of parameters and the replication and is lower than the standard correlation coefficient (Zar, 1996). P-values (F-test) of the significance of the overall fit are also reported. It is important the reader keep in mind that although Eq. 7 may look involved it represents in reality a simple measure of the eccentricity (Eq. 5/6) stretched or shrunk along both axes to adapt to and fit the range of real r-values. The fitting procedure was performed in Origin 8 Pro with Eq. 7 added as a custom non-linear function.

Results

Accepted manuscript

ACCEPTED MANUSCRIPT

Categorical orientation responses

Fig. 6 shows the three categorical orientation responses (normal, shifted, and disorientation) reported in the literature as a function of wavelength and irradiance. Cases of normal orientation are shown with black triangles, cases of shifted orientation are shown as open diamonds with a cross line, and cases of disorientation are shown as open circles. Overlapping data is shown by a cross at the original data point and the number of actual data is shown as dots on both sides of the cross. Fixed uni-modal responses has been taken as shifted orientation if they deviated from the normal direction by more than 45° and as normal if they deviated by less.

The arrows 1 – 4 in Fig. 6 suggest the very same trends exist in the real orientation data as those predicted by the model (c.f. Fig. 4; for ease of reference with Fig. 4 the arrows in Fig. 6 have been given the same categorical numbers (1-4)). Let us first look at cases where the wavelength is constant and the irradiance is changed. Along the right arrow assigned "1" around 565 nm the birds were seen to be predominately normally oriented below $20 \cdot 10^{15}$ quanta/m^2/s, between 20 and $35 \cdot 10^{15}$ quanta/m^2/s they were predominantly disoriented, from 35 to $55 \cdot 10^{15}$ quanta/m^2/s the birds were mainly shifted in their orientation, and at approximately $70 \cdot 10^{15}$ quanta/m^2/s there was both a case of expected disorientation and a single case of normal orientation not explainable by the model. Similarly, along the left arrow marked "1" at 424 nm the birds were normally oriented around $10 \cdot 10^{15}$ quanta/m^2/s, predominantly disoriented between approximately 30 and $40 \cdot 10^{15}$ quanta/m^2/s, then shifted in orientation just above $40 \cdot 10^{15}$ quanta/m^2/s, and disoriented again around $55 \cdot 10^{15}$ quanta/m^2/s but a case of normal orientation around $70 \cdot 10^{15}$ quanta/m^2/s not explainable by the model. In contrast, in tests around 500 nm the birds

Accepted manuscript

ACCEPTED MANUSCRIPT

showed normal orientation at all intensities from just below $10 \cdot 10^{15}$ quanta/m^2/s up to $70 \cdot 10^{15}$ quanta/m^2/s with just a single deviant case with shifted orientation (arrow 2; c.f. Fig. 4).

Now let us keep the irradiance constant and see what the data show when the wavelength is changed. Along the lowermost arrow assigned "3" in Fig. 6 at irradiances around $10 \cdot 10^{15}$ quanta/m^2/s it can be seen that from around 500 to 565 nm the orientation responses were predominantly normal, then around 590 nm the birds were all disoriented, at approximately 620 nm they were shifted 90° in their orientation, and between 625 and 650 nm they were again predominately disoriented. Along the upper arrow assigned "3" at an irradiance round $45 \cdot 10^{15}$ quanta/m^2/s the birds predominately showed normal orientation around 500 nm, there was no disorientation (possibly because of lacking data), but around 565 nm the birds were predominately shifted in their orientation, and around 600 nm and upwards the birds were disoriented. The two arrows marked "4" both suggest that the sequence of orientation responses were skewed towards lower irradiances when going from around 425 nm to 375 nm or from around 565 nm to around 625 nm as predicted by the model (see above and Fig. 4). In conclusion, the passerine literature shows a rather strong overall correlation in its pattern of orientation responses as a function of both wavelength and irradiance to those predicted by the model.

A predicted sequence of shifts in categorical orientation responses at a constant irradiance of $45 \cdot 10^{15}$ quanta/m^2/s (except $22 \cdot 10^{15}$ quanta/m^2/s at 400 nm) was also seen in data from the red-spotted newt (Tab. 1). The newts changed from normal orientation at 400 and 450 nm to disorientation at 475 nm and finally a 90^o shift at 500 nm. The data is

Accepted manuscript

ACCEPTED MANUSCRIPT

too sparse in the other species shown in Tab. 1 to take into consideration, but does not disagree with the model.

Concentration of orientation

Fig. 7 shows how r-values from the literature changed with irradiance at constant wavelengths (Fig. 7A-B) or with wavelength at approximate constant irradiances (Fig. 7C-D). Averages with standard deviation error bars are shown in cases where more than one data point was available, but all fits were performed on individual data points (sample size N is given in the figures). At a constant wavelength of 424 nm the cue integration model showed a good fit to available r-values with an R_{adj} value of 0.81 and $p = 0.0004$ (Fig. 7A). The point in the normal orientation category at highest irradiance (in brackets) seems to be a significant outlier both in value and orientation category and it was excluded from the analysis. Including the outlier gives the statistics $R_{adj} = 0.47$ and $p = 0.04$ which still is significant, but not surprisingly with a much lower R_{adj} value. There is evidence that polarization cues and possibly the correlated color gradients can be suppressed at high irradiances (Kinoshita et al., 2007) and in such case, the model would actually predict normal orientation. At a constant wavelength of 565 nm there was good fit of the model to the r-values with $R_{adj} = 0.74$ and $p < 0.0001$ (Fig. 7B). Again, the outlier at high irradiance was excluded with the same argument as above. Inclusion of the outlier results in the alternative statistics $R_{adj} = 0.67$ and $p < 0.0001$ which still is a rather good overall fit. At approximate constant irradiances a good fit was shown at an irradiance between $6 – 14 \cdot 10^{15}$ quanta/m^2/s with $R_{adj} = 0.93$ and $p < 0.0001$ (Fig. 7C) and at an approximate constant flux of $43 – 54 \cdot 10^{15}$ quanta/m^2/s with $R_{adj} = 0.74$ and $p < 0.001$ (Fig. 7D).

Accepted manuscript

ACCEPTED MANUSCRIPT

Data was also available for the red-spotted newt at a constant irradiance of $45 \cdot 10^{15}$ quanta/m^2/s (except $22 \cdot 10^{15}$ quanta/m^2/s at 400 nm). If the outlier at 600 nm was included in the analysis the fit is poor with R^2_{adj} = - 0.34 and p = 0.016 (R^2_{adj} is negative if the fit is very poor and the residual mean squares are larger than the total mean square (Zar, 1996)). If the outlier was masked from the analysis a fair fit is obtained with R_{adj} = 0.77 and p = 0.004. Since the latter analysis is more informative the summary of this analysis was included in Fig. 7E.

Finally, since the fitting procedure was done by simple scaling of a fixed curve form, each data point can be transformed back into the numerical domain of the model (spikes/s) independent of whether the data point originally is a function of irradiance or wavelength. This way, the overall fit of the model to all available literature data points can be assessed. As can be seen in Fig. 7F, the summarized overall fit to the total data was quite remarkable, in spite of the fact that the data were from different bird species, different studies, and/or originated as a function of irradiance or wavelength. Running a fit on the total data set gives a R_{adj} = 0.94 and $p << 0.0001$.

Spectral correlations

If the underlying visual compass is a color gradient compass we would expect disorientation and 90^o shifts in both the UV (or near UV) and longer wavelengths. In birds (were most data is present) this is the case and in general fits a model based on color gradient very well. The photoreceptors involved in passerines may be the UV sensitive (UVS) cones and/or possibly the short wavelength sensitive (SWS) for the UV/near UV mechanism (spectral sensitivities of typical passerine photoreceptors are shown in Fig. 6).

Accepted manuscript

ACCEPTED MANUSCRIPT

The LW mechanism may be mediated by the mid wavelength sensitive (MWS), double cones (DC), and/or long wavelength sensitive cones (LWS). If there is a reference color, the SWS, MWS, and/or rods seem to be possible candidates.

In the newts the pattern does not immediately fit the idea of a color gradient compass since orientation shifts are mainly observed in the MW-LW with no observations near the UV (Table 1). However, the newt has not been as extensively studied with several different irradiances as with the passerine birds, where it is evident, that very different results are to be expected at different irradiances. Tests with higher irradiance and further down in the UV may thus reveal patterns that allow a better comparison. Orientation by color gradients has already been documented in insects and they would provide good test animals for the model. Unfortunately, the light dependent orientation response data available for insects (Tab. 1) are too few and can be interpreted in too many ways to allow any meaningful statements.

Discussion

The current cue integration model explains the complex light-dependent orientation responses surprisingly well and provides an important alternative to the radical pair hypothesis as an explanation of these responses. It combines the questionable dual magnetic reception hypotheses (radical pair and magnetite) into one simple hypothesis that parsimoniously points to a single magneto-reception mechanism (probably based on IBMC) which through an integration process with a celestial compass can be interfered with by light. The literature data support the proposed cue integration model very well: the predicted sequence of categorical orientation shifts as a function of both irradiance and

Accepted manuscript

ACCEPTED MANUSCRIPT

wavelength match closely to those observed in the literature (Fig. 6) and model predictions on the concentration of orientation as a function of both irradiance and wavelength fits surprisingly well with observed r-values (Fig. 7).

Model performance

Although it has great explanatory power the model is crude in its current form. It has for instance a problem if both cues happen to be equal in all directions since the integration here will cancel to zero. Future elaborations are necessary if the model can be validated, but inappropriate to address further at the current stage. The model is very robust and will give very similar predictions and good fits within a wide range of the parameters A_{mag}, B_{mag}, and $SF(\omega)'_{col}$ that are far from limited to the arbitrary ones used. The model is not dependent on the elliptic form of $SF_{mag}(\omega)$ and will give very similar results with integration between any elongated form and the uniform circular distribution of $SF(\omega)'_{col}$.

The model is based on an assumption of lateral inhibition. Pragmatically, lateral inhibition is more complicated than simple subtraction (Golden, 1996). However, the model is robust and as long as the lateral inhibition function is linear and uniform in all geographical directions the same overall model pattern will emerge and result in similar predictions.

Future test of model validity

In the following I will present some suggestions on how to test the cue integration model with focus on the passerine birds. Unfortunately, since the presence and nature of a

Accepted manuscript

ACCEPTED MANUSCRIPT

color gradient sensory system is unknown in vertebrates it is difficult to suggest any direct test of the model.

The presence of a color gradient compass

First of all it will be important to establish if birds sense and are able to orient by skylight color gradients. This should be relatively easy to establish for instance by placing birds in the traditional test funnels covered by a frosted dome and set up color gradients by differential illumination. However, great care must be taken to exclude intensity cues (Coemans and Vos, 1992). The magnetic field has to be cancelled by Helmholtz coils to eliminate it as a compass cue.

Illumination with two or more monochromatic sources

The idea of testing birds in illumination by two or more different monochromatic light sources is a good one (Wiltschko et al., 2004a). Unfortunately, the results of Wiltschko et al (2004a) are difficult to interpret and the birds behaved different in autumn and spring. However, such types of experiments could be done to address some key characteristics of the cue integration model. There seems to be at least three different possible constitutions of a color gradient compass: 1) a compass that works without a reference color and is a simple UV/LW antagonism (Eq. 2; compass 1 in Tab. 2). 2) A compass that has UV/LW antagonism but uses a color in the SW-LW range as a reference (Eq. 3; compass 2 in Tab. 2) . 3) A color gradient compass with no UV/LW antagonism and with a color in the SW-MW range as a reference (compass 3 in Tab. 2):

Accepted manuscript

ACCEPTED MANUSCRIPT

534 $$SF(\omega)_{col} \approx \frac{|SF_{UV}(\omega) + SF_{LW}(\omega)|}{SF_{SW-MW}(\omega)}$$ (Equation 8)

535

536 (Equation X)The three different compasses will predict different
537 experimental outcomes in the mixed color conditions as shown in Tab. 2: **Experiment 1a:**
538 the initial condition in Exp. 1a is at a constant irradiance in the UV (around perhaps 375
539 nm) high enough to elicit disorientation (the final stage of disorientation (end of arrows 1 in
540 Fig. 4)). This is probably occurring at a constant illumination of $20 – 30 \cdot 10^{15}$ quanta/m^2/s.
541 In case of compass 1 and 2 the UV/LW antagonism will increasingly counteract each other
542 as the LW irradiance (~625 nm) is increased and the orientation will be predicted to change
543 from disorientation into shifted orientation, to disorientation, and eventually when the UV
544 and LW color antagonism cancel each other, the orientation becomes normal. The normal
545 orientation is therefore expected to happen when the sensitivity of the LW mechanism
546 (S_{LW}) approximates that of the UV mechanism at $20 – 30 \cdot 10^{15}$ quanta/m^2/s ($S_{UV.20\text{-}30}$) and
547 will give an estimate of the relative sensitivities of the UV and LW mechanisms. In the case
548 of compass 3 with no UV/LW antagonism the orientation response is expected to be
549 constant disorientation. **Experiment 1b:** in case of compass 1 and 2 the opposite sequence
550 of orientation responses ($N \rightarrow D \rightarrow S \rightarrow D$) of Exp. 1a is expected to be observed as the
551 LW irradiance is increased from $S_{LW} = S_{UV.20\text{-}30}$ to $S_{LW} = 2 \cdot S_{UV.20\text{-}30}$ (given the system is
552 linear). However, disorientation is again expected throughout for compass 3. **Experiment**
553 **2:** in case of compass 1 and 2, the initial condition here is the one found in Exp. 1 where the
554 sensitivity of the LW mechanism is the same as that of the UV mechanism at $20 – 30 \cdot 10^{15}$
555 quanta/m^2/s ($S_{LW} = S_{UV.20\text{-}30}$) and the orientation is normal. If the irradiance in the SW-MW

Accepted manuscript

ACCEPTED MANUSCRIPT

range (~500 nm) is increased the orientation will stay normal for compass 1 and 2 since the UV and LW mechanisms will always be cancelled out. However, for compass 3 with no UV/LW antagonism, the orientation will be expected to be disorientation in the initial condition, but expected to show a $D \rightarrow S \rightarrow D \rightarrow N$ sequence of orientation responses as the increasing SW-MW irradiance increasingly reduces $SF(\omega)_{col}$ (obviously it is not possible to establish $S_{LW} = S_{UV.20\text{-}30}$ as with compass 1 and 2 for compass 3, and here, an illumination of $15 \cdot 10^{15}$ quanta/m^2/s in both the UV and LW will probably be suitable and result in disorientation). **Experiment 3:** here all compasses are predicted to show an initial orientation response of disorientation. As the SW-MW irradiance is increased compass 1 predicts constant disorientation since it has no reference color and the UV/LW contrast will stay constant. Oppositely, compasses 2-3 with reference detectors will be expected to show the $D \rightarrow S \rightarrow D \rightarrow N$ sequence. **Experiment 4:** seems trivial and will not help separate the compasses, but predicts that the typical normal orientation observed at irradiances of, for instance, 15 quanta/m^2/s (Fig. 6) is not due to a mechanism that depends on this wavelength to function for normal magneto reception and that once saturated will continue to function normally regardless of the presence of other wavelength light (as would be the logical consequence of a cryptochrome based radical pair magnetic compass), but is part of a system that is dependent on the relative balance between wavelengths as is the case in the proposed cue integration model.

As follows from the above and Tab. 2, performance of Exp. 1-4 can help establish whether or not a group of test birds will show behaviors that are consistent with the model predictions. Although it may not provide direct evidence, positive results will strongly

Accepted manuscript

ACCEPTED MANUSCRIPT

support the cue integration model. Especially so if the existence of a color gradient compass can be demonstrated at the same time. Exp. 1-3 will help determine what type of compass (1-3) lies behind the integration process.

A possible role of a polarization compass?

Although the simplicity of the color gradient compass highly favors it as the major candidate in the model, there is a theoretical possibility of an alternative role of a polarization compass which deserves mentioning. In polarization sensitivity two orthogonally oriented polarization receptors and a luminosity detector is sufficient to determine the three important factors: total intensity (I), e-vector orientation (φ) and degree of polarization (d) (Bernard and Wehner, 1977; Flamarique and Hawryshyn, 1998; Wehner, 1983; Wehner et al., 1975). If the detectors have separate spectral sensitivities, a compass based on the degree of polarization and/or e-vector orientation may lead to misperceptions similar to those proposed for the color gradient compass. In support of this, polarization vision in many animals may not always be entirely independent of color. In vertebrates, some fishes show clear evidence of the use of different color sensitive cones (UV and LW sensitive) in polarization vision (Cameron and Easter, 1993; Coughlin and Hawryshyn, 1995; Hawryshyn and McFarland, 1987; Parkyn and Hawryshyn, 1993), although here, it has been concluded that color is unlikely to confound with polarization sensitivity (Ramsden et al., 2008). In invertebrates, *Daphnia pulex* show wavelength dependent polarization vision and shift their orientation 90˚ relative to the normal angular direction in polarized light of wavelengths above 570 nm, they are disoriented in polarized light of wavelengths above 515 nm, whereas they keep their orientation normal in polarized light of

Accepted manuscript

ACCEPTED MANUSCRIPT

600 wavelengths above 455 nm (Flamarique and Browman, 2000). In the locust (*Schistocerca*
601 *gregaria*) polarization sensitive neurons respond differently to both unpolarized UV and
602 green light, and polarized blue light indicating different roles of spectrally different units in
603 polarization related vision (Kinoshita et al., 2007). Papilio butterflies show polarization
604 vision that is dependent on colors and anatomical and physiological data has been pointed
605 out to suggest an interdependence of polarization and color vision in other species like
606 Pieris and Nymphalid butterflies, tabanid flies (*Tabanidae*), ladybirds (*Coccinella*
607 *septempunctata*), and Waterstriders (*Gerris palludum*) (Kelber et al., 2001).

608 ## Acknowledgements

609 I dedicate this work to my parents Poul Jensen and Joan Kragh Jensen, to my two
610 kids Tinus Michel Kragh Jensen and Lara Michel Kragh Jensen, and to my wife Meredith
611 Leigh Jensen. I thank Ole Næsbye Larsen, Henrik Mouritsen, Rachel Muheim, and
612 Wolfgang Wiltschko for comments on earlier crude drafts in 2001 – 2002. I thank John B.
613 Phillips and Michael Walker for comments on more recent drafts in 2008. I thank Almut
614 Kelber and Uwe Homberg very much for valuable critique of parts related to vision. I thank
615 Meredith Leigh Jensen for language corrections. Finally I thank the three reviewers for
616 comments leading to great improvements of the manuscript. Part of this work was
617 performed while being supported by a grant from Carlsbergfondet (2006_01_0513) and a
618 grant from the Danish National Research Foundation awarded to the Center of Sound
619 Communication.

620 ## Appendix

Accepted manuscript

ACCEPTED MANUSCRIPT

// Dear editors and reviewers. The appendix consist of no text and only of two figures (figures texts are below) that I think is an important elaboration on technical parts of the fitting procedure to convince the reader that the fitting is in principle very simple and that the parameters does not change the curve form per se.//

Figure A1: Comparison of the traditional eccentricity (Eq. 5) and the modified eccentricity (Eq. 6). As can be seen the two curves come very close. The modified eccentricity was introduced to automate and improve the fitting procedure by avoiding problems with square roots of negative numbers when the model orientation shifts by 90˚. The modified eccentricity equation may prove especially helpful in future experiments when more data is available or data is collected aimed at direct tests of the model so that fits can be made to evaluate model parameters in a more precise way.

Figure A2: Demonstrates how various parameters of the modified eccentricity fitting equation affect the fitting curve. **A)** The parameter *k* of Eq. 7 mainly shifts the curve along the abscissa without compressing the curve much. **B)** The parameter *m* mainly compresses the curve so that for instance the slope of the decreasing eccentricity at the end of the curve increases. **C)** The parameter *n* scales the curve along the ordinate. **D)** Given that A_{mag} is fixed the parameter B_{mag} determines the eccentricity and precision of the model magnetic compass itself (see Eq. 1 & 6) and determines the eccentricity at $SF(\omega)^{\circ}_{est} = 0$.

Table and Figure Legends

Accepted manuscript

ACCEPTED MANUSCRIPT

642 **Table 1:** Light-dependent orientation responses in non-passerine birds, amphibians, and
643 insects. *N* = normal orientation towards an expected and meaningful direction, *D* =
644 disorientation, *S* = shifted orientation 90° in relation to the normal orientation. The
645 wavelength of the monochromatic light is shown at the top and the numbers show the
646 irradiance in 10^{15} quanta/m^2/s. (Data taken from Freake and Phillips, 2005; Phillips and
647 Borland, 1992a; Phillips and Borland, 1992b; Phillips and Sayeed, 1993; Vacha et al.,
648 2008; Wiltschko and Wiltschko, 1998; Wiltschko et al., 2007b).
649
650 **Table 2:** Expected orientation responses predicted by the cue integration model in different
651 orientation tests with illumination by two to three different monochromatic light sources.
652 See text for details.
653
654 **Figure 1:** Hypothetical model compasses. **A)** A hypothetical magnetic compass consisting
655 of a circular array of cells. Cell spike frequency is coded by gray scale such that the darker
656 the cell the more excited it is. The directional firing pattern (see text) is represented
657 mathematically as radial plots of spike frequencies forming an ellipse (middle). **B)** A
658 simplified 2D hypothetical color gradient compass. The compass consists of a circular array
659 of cells receiving input from photoreceptors that sample the horizon around all 360˚.
660 Scattering of sunlight on the atmosphere result in a skylight color gradient with a relative
661 high amount of long wavelength light in direction of the sun (light grey part of the
662 outermost circle) and a relative high amount of UV light (or shorter wavelengths in general)
663 in the anti solar direction (dark grey part of the outermost circle). In the solar and anti solar
664 direction (solar meridian) the difference in the irradiance of long wavelength and UV is

Accepted manuscript

ACCEPTED MANUSCRIPT

665 therefore greatest. This difference is assumed to excite the compass cells (see text) and the
666 cells aligned along the solar meridian are therefore maximally excited whereas there's a
667 minimal excitation in directions 90 relative to the solar meridian. The directional firing
668 pattern is therefore represented as an ellipse (middle) like in A. (grayscale code of compass
669 cells as in A). **C)** If the hypothetical compass sensory system in B is placed in
670 monochromatic light within a wavelength that specifically excites the long wavelength or
671 UV detectors only, the sensory system will perceive a large difference in long wavelength
672 and UV light in all directions all units will be highly excited (all units are dark gray). The
673 resultant directional firing pattern is thus forming a circle rather than an ellipse.
674
675 **Figure 2:** Model integration (solid line) between the hypothetical magnetic compass
676 (dotted line) and the hypothetical color gradient compass (dashed line). Major and minor
677 compass axes are arbitrarily set to 70 spikes/s and 35 spikes/s, and 100 spikes/s and 35
678 spikes/s for the magnetic and color gradient compass, respectively (see text). **A)** The
679 integration leads to a compass with a higher contrast between the North-South and East-
680 West axes. **B)** If, for instance, the two cues are misaligned (here by 15°) the hypothetical
681 integration compass will show a clear direction along the axis of the most prominent cue.
682
683 **Figure 3:** The outcome of the integration process in monochromatic light at different radial
684 spike frequency values, $SF(\omega)^{\circ}_{col}$, of the color gradient (*dashed line*). *Dotted line* =
685 magnetic compass, *solid line* = integrated compass. **A)** At low input ($SF(\omega)^{\circ}_{col} = 20$) into
686 the color gradient compass (e.g. low intensity of the monochromatic light; see text) there is

Accepted manuscript

ACCEPTED MANUSCRIPT

only a little effect and the animals are still normally oriented. **B)** As the input increases ($SF(\omega)'_{col} = 52$) the resultant integrated compass has significant lobes along both axes presumably resulting in disorientation. **C)** As the input further increases ($SF(\omega)'_{col} = 75$) the East-West axis starts dominating and the result is a 90˚ orientation shift of the animals. **D-E)** The more the input into the color gradient compass increases from here ($SF(\omega)'_{col} = 150$ and 400), the more the contrast between the East-West and North-South axis deteriorates and the animals will be expected to show disorientation again.

Figure 4: Categorical orientation responses as a function of light wavelength and irradiance. The model predicted orientation responses are outlined together with hypothetical absorption spectra (thick solid lines) of the hypothetical color gradient system assumed to be consisting of UV and LW sensitive detectors. The arrows show predictions of sequences of orientation responses. *N* = normal orientation, *D* = disorientation, and *S* = shifted orientation. See text for details.

Figure 5: Model predicted changes in eccentricity (Eq. 5) of the integrated compass as the circular excitation of the color gradient compass, $SF(\omega)'_{col}$, increases. The higher the eccentricity, the better the integrated compass points out directions. Shown are also references to Fig. 3 in which the corresponding directional firing pattern of the integrated compass can be seen. *Solid line* = predicted normal orientation, *dotted line* = predicted

Accepted manuscript

ACCEPTED MANUSCRIPT

707 disorientation, and *dashed line* = predicted shifted orientation. Calculated with A_{mag} = 70
708 and B_{mag} = 35.
709
710 **Figure 6:** The literature data on orientation responses of passerines under monochromatic
711 light of different wavelengths and irradiances. Shown is also the normalized photon catches
712 of visual cones from a representative passerine, the blue tit (*Parus caeruleus*), including oil
713 droplet absorption (*UVS* = ultraviolet sensitive cones, *SWS* = short wave sensitive cones,
714 *MWS* = mid wave sensitive cones and *LWS* = long wave sensitive cones). The normalized
715 absorption spectrum of rods (*RODS*) and the LWS pigments present in double cones (*DC*;
716 double cones generally lack oil droplets) are also shown. Shifted orientation (*open*
717 *diamonds with a cross line*) includes both observed 90° shifted bimodal orientation and
718 unimodal so-called "fixed orientations" of these deviated 45° or more from the normal
719 orientation. Overlapping data points are shown as a horizontal row of points and their
720 common origin shown with a cross. The numbered arrows indicate trends of orientation
721 shifts that were predicted by the model as shown in Fig. 4. Vision data for single cones was
722 taken from Hart and Hunt (2007). Double cone absorption spectrum was calculated from
723 Govardovskii et al (2000) with no oil droplet correction. Orientation data was taken from
724 (Stapput (2006) doctorial thesis data referenced in: Johnsen et al., 2007; Muheim et al.,
725 2002a; Munro et al., 1997; Rappl et al., 2000; Wiltschko et al., 2007a; Wiltschko et al.,
726 2005; Wiltschko et al., 2008; Wiltschko and Wiltschko, 1995b; Wiltschko and Wiltschko,
727 1999b; Wiltschko and Wiltschko, 2000; Wiltschko and Wiltschko, 2001; Wiltschko and
728 Wiltschko, 2002; Wiltschko and Wiltschko, 2005; Wiltschko et al., 2000; Wiltschko et al.,

Accepted manuscript

ACCEPTED MANUSCRIPT

729 2001; Wiltschko et al., 1993; Wiltschko et al., 2003; Wiltschko et al., 2004a; Wiltschko et
730 al., 2004b).
731
732 **Figure 7:** Model fits of compass eccentricity to literature r-values at wavelengths or
733 irradiances where adequate data were available. Statistics of the fits are summarized in each
734 figure (see methods for details). Compass eccentricity fitted to literature r-values of birds as
735 a: **A)** function of irradiance at a constant wavelength of 424 nm. **B)** function of irradiance at
736 a constant wavelength of 565 nm. **C)** function of wavelength within a constant range of
737 irradiances between $6 – 14 \cdot 10^{15}$ quanta/m^2/s. **D)** function of wavelength within a constant
738 range of irradiances between $43 – 54 \cdot 10^{15}$ quanta/m^2/s. **E)** Compass eccentricity fitted to
739 literature r-values of red-spotted newts as a function of wavelength at a constant
740 irradiances of $45 \cdot 10^{15}$ quanta/m^2/s (except $22 \cdot 10^{15}$ quanta/m^2/s at 400 nm). **F)** Summary
741 of all fits to the bird data. Each data point was transferred back into the numerical domain
742 of the model by a transformation based on the values of the parameters *n*, *k*, and *m* of the
743 fitting curve.

744 References

745 Able, K.P., 1991. Common themes and variations in animal orientation systems. Am. Zool.
746 31, 157-167.
747 Adair, R.K., 1999. Effects of very weak magnetic fields on radical pair reformation.
748 Bioelectromagnetics 20, 255-263.
749 Batschelet, E., 1981. Circular Statistics in Biology. Academic Press, London.

Accepted manuscript

ACCEPTED MANUSCRIPT

750 Beason, R.C., and Nichols, J.E., 1984. Magnetic orientation and magnetically sensitive
751 material in a transequatorial migratory bird. Nature 309, 151-153.
752 Bernard, G.D., and Wehner, R., 1977. Functional similarities between polarization vision
753 and color vision. Vis. Res. 17, 1019-1028.
754 Cameron, D.A., and Easter, S.S., 1993. The cone photoreceptor mosaic of the green sunfish
755 (*Leomis cyanellus*). Visual Neurosci. 10, 375-384.
756 Cintolesi, F., Ritz, T., Kay, C.W.M., Timmel, C.R., and Hore, P.J., 2003. Anisotropic
757 recombination of an immobilized photoinduced radical pair in a 50-mu T magnetic
758 field: a model avian photomagnetoreceptor. Chem. Phys. 294, 385-399.
759 Coemans, M.A.J.M., and Vos, J., On the perception of polarized light by the homing
760 pigeon, Biological faculty, University of Utrecht 1992, pp. 1-190.
761 Coemans, M.A.J.M., Hzn, J.J.V., and Nuboer, J.F.W., 1994. The relationship between
762 celestial color gradients and the position of the sun with regard to the sun compass.
763 Vis. Res. 34, 1461-1470.
764 Coughlin, D.J., and Hawryshyn, C.W., 1995. A cellular basis for polarized light vision in
765 rainbow trout. J. Comp. Physiol. A 176, 261-272.
766 Davila, A.F., Fleissner, G., Winklhofer, M., and Petersen, N., 2003. A new model for a
767 magnetoreceptor in homing pigeons based on interacting clusters of
768 superparamagnetic magnetite. Phys. Chem. Earth 28, 647-652.
769 Davila, A.F., Winklhofer, M., Shcherbakov, V.P., and Petersen, N., 2005. Magnetic pulse
770 affects a putative magnetoreceptor mechanism. Biophys. J. 89, 56-63.
771 Deutschlander, M.E., Phillips, J.B., and Borland, S.C., 1999. The case for light-dependent
772 magnetic orientation in animals. J. Exp. Biol. 202, 891-908.

Accepted manuscript

ACCEPTED MANUSCRIPT

773 Diebel, C.E., Proksch, R., Green, C.R., Neilson, P., and Walker, M.M., 2000. Magnetite
774 defines a vertebrate magnetoreceptor. Nature 406, 299-302.
775 Edmonds, D.T., 1992. A magnetite null detector as the migrating bird's compass. Proc.
776 Roy. Soc. Lond. B 249, 27-31.
777 Efimova, O., and Hore, P.J., 2008. Role of exchange and dipolar interactions in the radical
778 pair model of the avian magnetic compass. Biophys. J. 94, 1565-1574.
779 Flamarique, I.N., and Hawryshyn, C.W., 1998. The common white sucker (Catostomus
780 commersoni): a fish with ultraviolet sensitivity that lacks polarization sensitivity. J.
781 Comp. Physiol. A 182, 331-341.
782 Flamarique, I.N., and Browman, H.I., 2000. Wavelength-dependent polarization orientation
783 in Daphnia. J. Comp. Physiol. A 186, 1073-1087.
784 Fleissner, G., Stahl, B., Thalau, P., Falkenberg, G., and Fleissner, G., 2007. A novel
785 concept of Fe-mineral-based magnetoreception: histological and physicochemical
786 data from the upper beak of homing pigeons. Naturwissenschaften 94, 631-642.
787 Fleissner, G., Holtkamp-Rotzler, E., Hanzlik, M., Winklhofer, M., Fleissner, G., Petersen,
788 N., and Wiltschko, W., 2003. Ultrastructural analysis of a putative magnetoreceptor
789 in the beak of homing pigeons. J. Comp. Neurol. 458, 350-360.
790 Freake, M.J., and Phillips, J.B., 2005. Light-dependent shift in bullfrog tadpole magnetic
791 compass orientation: Evidence for a common magnetoreception mechanism in
792 anuran and urodele amphibians. Ethology 111, 241-254.
793 Golden, R.M., 1996. Mathematical Methods for Neural Network Analysis and Design. MIT
794 Press.

Accepted manuscript

ACCEPTED MANUSCRIPT

795 Govardovskii, V.I., Fyhrquist, N., Reuter, T., Kuzmin, D.G., and Donner, K., 2000. In
796 search of the visual pigment template. Visual Neurosci. 17, 509-528.
797 Hanzlik, M., Heunemann, C., Holtkamp-Rotzler, E., Winklhofer, M., Petersen, N., and
798 Fleissner, G., 2000. Superparamagnetic magnetite in the upper beak tissue of
799 homing pigeons. Biometals 13, 325-331.
800 Hart, N.S., and Hunt, D.M., 2007. Avian visual pigments: characteristics, spectral tuning,
801 and evolution. Am. Nat. 169, S7-S26.
802 Hawryshyn, C.W., and McFarland, W.N., 1987. Cone photoreceptor mechanisms and the
803 detection of polarized light in fish. J. Comp. Physiol. A 160, 459-465.
804 Johnsen, S., and Lohmann, K.J., 2005. The physics and neurobiology of magnetoreception.
805 Nature Reviews Neuroscience 6, 703-712.
806 Johnsen, S., and Lohmann, K.J., 2008. Magnetoreception in animals. Phys. Today 61, 29-
807 35.
808 Johnsen, S., Mattern, E., and Ritz, T., 2007. Light-dependent magnetoreception: quantum
809 catches and opponency mechanisms of possible photosensitive molecules. J. Exp.
810 Biol. 210, 3171-3178.
811 Kelber, A., Thunell, C., and Arikawa, K., 2001. Polarisation-dependent colour vision in
812 Papilio butterflies. J. Exp. Biol. 204, 2469-2480.
813 Kinoshita, M., Pfeiffer, K., and Homberg, U., 2007. Spectral properties of identified
814 polarized-light sensitive interneurons in the brain of the desert locust Schistocerca
815 gregaria. J. Exp. Biol. 210, 1350-1361.
816 Kirschvink, J.L., and Gould, J.L., 1981. Biogenic magnetite as a basis for magnetic field
817 detection in animals. Biosystems 13, 181-201.

Accepted manuscript

ACCEPTED MANUSCRIPT

818 Kirschvink, J.L., and Walker, M.M., Particle-size considerations for magnetite-based
819 magnetoreceptors, in: Kirschvink, J. L., et al., Eds.), Magnetite Biomineralization
820 and Mangetoreception in Organisms: A New Biomagnetism, Vol. 1. Plenum Press,
821 New York & London 1985, pp. 243-254.
822 Maeda, K., Henbest, K.B., Cintolesi, F., Kuprov, I., Rodgers, C.T., Liddell, P.A., Gust, D.,
823 Timmel, C.R., and Hore, P.J., 2008. Chemical compass model of avian
824 magnetoreception. Nature 453, 387-U38.
825 Mouritsen, H., 1998. Redstarts, Phoenicurus phoenicurus , can orient in a true-zero
826 magnetic field. Anim. Behav. 55, 1311-1324.
827 Muheim, R., 2006. Magnetic compass calibration: a single calibration reference derived
828 from sunset/sunrise polarized light cues from the region of sky near the horizon? J.
829 Ornithol. 147, 50-50.
830 Muheim, R., Backman, J., and Akesson, S., 2002a. Magnetic compass orientation in
831 European robins is dependent on both wavelength and intensity of light. J. Exp.
832 Biol. 205, 3845-3856.
833 Muheim, R., Bäckman, J., and Åkesson, S., Magnetic compass orientation in European
834 robins is dependent on both wavelength and intensity of light, Bird Orientation:
835 External Cues and Ecological Factors, Lund University 2002b, pp. 162 pp.
836 Munro, U., Munro, J.A., Phillips, J.B., and Wiltschko, W., 1997. Effect of wavelength of
837 light and pulse magnetisation on different magnetoreception systems in a migratory
838 bird. Austr. J. Zool. 45, 189-198.

Accepted manuscript

ACCEPTED MANUSCRIPT

839 Parkyn, D.C., and Hawryshyn, C.W., 1993. Polarized light sensitivity in rainbow trout
840 (*Oncorhyncus mukiss*) - characterization from multiunit responses in the optic
841 nerve. J. Comp. Physiol. A 172, 493-500.
842 Phillips, J.B., and Borland, S.C., 1992a. Behavioural evidence for use of a light-dependent
843 magnetoreception mechanism by a vertebrate. Nature 359, 142-144.
844 Phillips, J.B., and Borland, S.C., 1992b. Wavelength specific effects of light on magnetic
845 compass orientation of the eastern red-spotted newt *Notophthalmus viridescens*
846 Ethol. Ecol. & Evol. 4, 33-42.
847 Phillips, J.B., and Sayeed, O., 1993. Wavelength-dependent effects of light on magnetic
848 compass orientation in Drosophila melanogaster J. Comp. Physiol. A 172, 303-308.
849 Ramsden, S.D., Anderson, L., Mussi, M., Kamermans, M., and Hawryshyn, C.W., 2008.
850 Retinal processing and opponent mechanisms mediating ultraviolet polarization
851 sensitivity in rainbow trout (*Onchorhynchus mykiss*). J. Exp. Biol. 211, 1376-1385.
852 Rappl, R., Wiltschko, R., Weindler, P., Berthold, P., and Wiltschko, W., 2000. Orientation
853 behavior of Garden Warblers (*Sylvia borin*) under monochromatic light of various
854 wavelengths. Auk 117, 256-260.
855 Ritz, T., Adem, S., and Schulten, K., 2000. A model for photoreceptor-based
856 magnetoreception in birds. Biophys. J. 78, 707-718.
857 Rodgers, C.T., and Hore, P.J., 2009. Chemical magnetoreception in birds: The radical pair
858 mechanism. PNAS 106, 353-360.
859 Rossel, S., and Wehner, R., 1984. Celestial orientation in bees - the use of spectral cues. J.
860 Comp. Physiol. A 155, 605-613.

Accepted manuscript

ACCEPTED MANUSCRIPT

861 Sancar, A., 1999. Cryptochromes as circadian photoreceptors in man and mouse.
862 Photochem. Photobiol. 69, 5S-5S.
863 Sancar, A., 2003. Structure and function of DNA photolyase and cryptochrome blue-light
864 photoreceptors. Chem. Rev. 103, 2203-2237.
865 Schulten, K., Magnetic field effects in chemistry and biology, Festkörperprobleme XXII,
866 1982, pp. 61-83.
867 Schulten, K., Windemuth, A., and Maret, G., Model for a physiological magnetic compass,
868 in: Boccara, N., (Ed.), Biophysical Effects of Steady Magnetic Fields, Springer-
869 Verlag Berlin, Heidelberg, New York, London, Paris, Tokyo 1986, pp. 99-106.
870 Shcherbakov, V.P., and Winklhofer, M., 1999. The osmotic magnetometer: a new model
871 for magnetite-based magnetoreceptors in animals. Eur. Biophys. J. Biophy. 28, 380-
872 392.
873 Solov'yov, I.A., and Greiner, W., 2007. Theoretical analysis of an iron mineral-based
874 magnetoreceptor model in birds. Biophys. J. 93, 1493-1509.
875 Solov'yov, I.A., and Greiner, W., 2008. Iron-mineral-based magnetoreceptor in birds:
876 polarity or inclination compass? European Physical Journal D 51, 161-172.
877 Solov'yov, I.A., and Schulten, K., 2009. Magnetoreception through Cryptochrome May
878 Involve Superoxide. Biophys. J. 96, 4804-4813.
879 Solov'yov, I.A., Chandler, D.E., and Schulten, K., 2007. Magnetic field effects in
880 Arabidopsis thaliana cryptochrome-1. Biophys. J. 92, 2711-2726.
881 Vacha, M., Puzova, T., and Drstkova, D., 2008. Effect of light wavelength spectrum on
882 magnetic compass orientation in Tenebrio molitor. J. Comp. Physiol. A 194, 853-
883 859.

Accepted manuscript

ACCEPTED MANUSCRIPT

884 Walker, M.M., 2008. A model for encoding of magnetic field intensity by magnetite-based
885 magnetoreceptor cells. J. Theor. Biol. 250, 85-91.
886 Walker, M.M., Diebel, C.E., Haugh, C.V., Pankhurst, P.M., Montgomery, J.C., and Green,
887 C.R., 1997. Structure and function of the vertbrate magnetic sense. Nature 390, 371-
888 376.
889 Wang, K., Mattern, E., and Ritz, T., 2006. On the use of magnets to disrupt the
890 physiological compass of birds. Phys. Biol. 3, 220-231.
891 Weaver, J.C., Vaughan, T.E., and Astumian, R.D., 2000. Biological sensing of small field
892 differences by magnetically sensitive chemical reactions. Nature 405, 707-709.
893 Wehner, R., The perception of polarised light, in: Cosens, D. J. and Vince-Prue, D., Eds.),
894 The Biology of Photo Reception, Cambridge University Press, Cambridge 1983.
895 Wehner, R., The ant's celestial compass system: spectral and polarization channels, in:
896 Lehrer, M., (Ed.), *Orientation and Communication in Arthropods*, Birkhäuser,
897 Basel 1997, pp. 145-185.
898 Wehner, R., Bernard, G.D., and Geiger, E., 1975. Twisted and non-twisted rhabdoms and
899 their significance for polarization detection in the bee. J. Comp. Physiol. A 104,
900 225-245.
901 Williams, M.N., and Wild, J.M., 2001. Trigeminally innervated iron-containing structures
902 in the beak of homing pigeons, and other birds. Brain Research 889, 243-246.
903 Wiltschko, R., and Wiltschko, W., 1995a. Magnetic orientation in animals. Springer,
904 Berlin.
905 Wiltschko, R., and Wiltschko, W., 1998. Pigeon homing: Effect of various wavelengths of
906 light during displacement. Naturwissenschaften 85, 164-167.

Accepted manuscript

ACCEPTED MANUSCRIPT

907 Wiltschko, R., and Wiltschko, W., 1999a. The orientation system of birds - I. Compass
908 mechanisms. J. Ornithol. 140, 1-40.
909 Wiltschko, R., and Wiltschko, W., 2006. Magnetoreception. Bioessays 28, 157-168.
910 Wiltschko, R., Wiltschko, W., Davies, M.N.O., and Green, P.R., Avian orientation:
911 Multiple sensory cues and the advantage of redundancy, Perception and Motor
912 Control in Birds, Springer-Verlag, Berlin Heidelberg 1994, pp. 95-119.
913 Wiltschko, R., Stapput, K., Bischof, H.J., and Wiltschko, W., 2007a. Light-dependent
914 magnetoreception in birds: increasing intensity of monochromatic light changes the
915 nature of the response. Front. Zool. 4, doi:10.1186/1742-9994-4-5.
916 Wiltschko, R., Ritz, T., Stapput, K., Thalau, P., and Wiltschko, W., 2005. Two different
917 types of light-dependent responses to magnetic fields in birds. Curr. Biol. 15, 1518-
918 1523.
919 Wiltschko, R., Munro, U., Ford, H., Stapput, K., and Wiltschko, W., 2008. Light-dependent
920 magnetoreception: orientation behaviour of migratory birds under dim red light. J.
921 Exp. Biol. 211, 3344-3350.
922 Wiltschko, W., The influence of magnetic total intensity and inclination on directions
923 preferred by migrating European Robins (*Erithacus rubecula*), in: Galler, S. R., et
924 al., Eds.), Animal Orientation and Navigation, NASA SP, Washington D.C. 1972,
925 pp. 569-578.
926 Wiltschko, W., and Wiltschko, R., 1993. Navigation in birds and other animals. J. Nav. 46,
927 174-191.

Accepted manuscript

ACCEPTED MANUSCRIPT

928 Wiltschko, W., and Wiltschko, R., 1995b. Migratory orientation of European robins is
929 affected by the wavelength as well as by a magnetic pulse. J. Comp. Physiol. A 177,
930 363-369.
931 Wiltschko, W., and Wiltschko, R., 1999b. The effect of yellow and blue light on magnetic
932 compass orientation in European robins, Erithacus rubecula J. Comp. Physiol. A
933 184, 295-299.
934 Wiltschko, W., and Wiltschko, R., 2000. Light-dependent magnetoreception in birds: Does
935 directional information change with light intensity? Naturwissenschaften 87, 36-40.
936 Wiltschko, W., and Wiltschko, R., 2001. Light-dependent magnetoreception in birds: the
937 behaviour of European robins, *Erithacus rubecula*, under monochromatic light of
938 various wavelengths and intensities. J. Exp. Biol. 204, 3295-3302.
939 Wiltschko, W., and Wiltschko, R., 2002. Magnetic compass orientation in birds and its
940 physiological basis. Naturwissenschaften 89, 445-452.
941 Wiltschko, W., and Wiltschko, R., 2005. Magnetic orientation and magnetoreception in
942 birds and other animals. J. Comp. Physiol. A 191, 675-693.
943 Wiltschko, W., Wiltschko, R., and Munro, U., 2000. Light dependent magnetoreception in
944 birds: the effect of intensity of 565-nm green light. Naturwissenschaften 87, 366-
945 369.
946 Wiltschko, W., Gesson, M., and Wiltschko, R., 2001. Magnetic compass orientation of
947 European robins under 565 nm green light. Naturwissenschaften 88, 387-390.
948 Wiltschko, W., Munro, U., Ford, H., and Wiltschko, R., 1993. Red light disrupts magnetic
949 orientation of migratory birds. Nature 364, 525-527.

Accepted manuscript

ACCEPTED MANUSCRIPT

950 Wiltschko, W., Munro, U., Ford, H., and Wiltschko, R., 2003. Magnetic orientation in
951 birds: non-compass responses under monochromatic light of increased intensity.
952 Proc. Roy. Soc. Lond. B 270, 2133-2140.
953 Wiltschko, W., Gesson, M., Stapput, K., and Wiltschko, R., 2004a. Light-dependent
954 magnetoreception in birds: interaction of at least two different receptors.
955 Naturwissenschaften 91, 130-134.
956 Wiltschko, W., Moller, A., Gesson, M., Noll, C., and Wiltschko, R., 2004b. Light-
957 dependent magnetoreception in birds: analysis of the behaviour under red light after
958 pre-exposure to red light. J. Exp. Biol. 207, 1193-1202.
959 Wiltschko, W., Freire, R., Munro, U., Ritz, T., Rogers, L., Thalau, P., and Wiltschko, R.,
960 2007b. The magnetic compass of domestic chickens, Gallus gallus. J. Exp. Biol.
961 210, 2300-2310.
962 Winklhofer, M., Holtkamp-Rotzler, E., Hanzlik, M., Fleissner, G., and Petersen, N., 2001.
963 Clusters of superparamagnetic magnetite particles in the upper-beak skin of homing
964 pigeons: evidence of a magnetoreceptor? Eur. J. Mineral. 13, 659-669.
965 Yorke, E.D., 1979. A possible magnetic transducer in birds. J. Theor. Biol. 77, 101-105.
966 Yorke, E.D., 1981. Sensivity of pigeons to small magnetic field variations. J. Theor. Biol.
967 89, 533-537.
968 Yorke, E.D., Kirschvink, J.L., Jones, D.S., and MacFadden, B.J., Energetics and sensivity
969 considerations of ferromagnetic magnetoreceptors, in: Stehli, F. G., (Ed.), Magnetite
970 Biomineralization and Mangetoreception in Organisms: A New Biomagnetism, Vol.
971 1. Plenum Press, New York & London 1985, pp. 233-242.
972 Zar, J.H., 1996. Biostatistical analysis. Prentice-Hall, Inc., Upper Saddle River, N.J. USA.

Accepted manuscript

ACCEPTED MANUSCRIPT

FIGURE 1

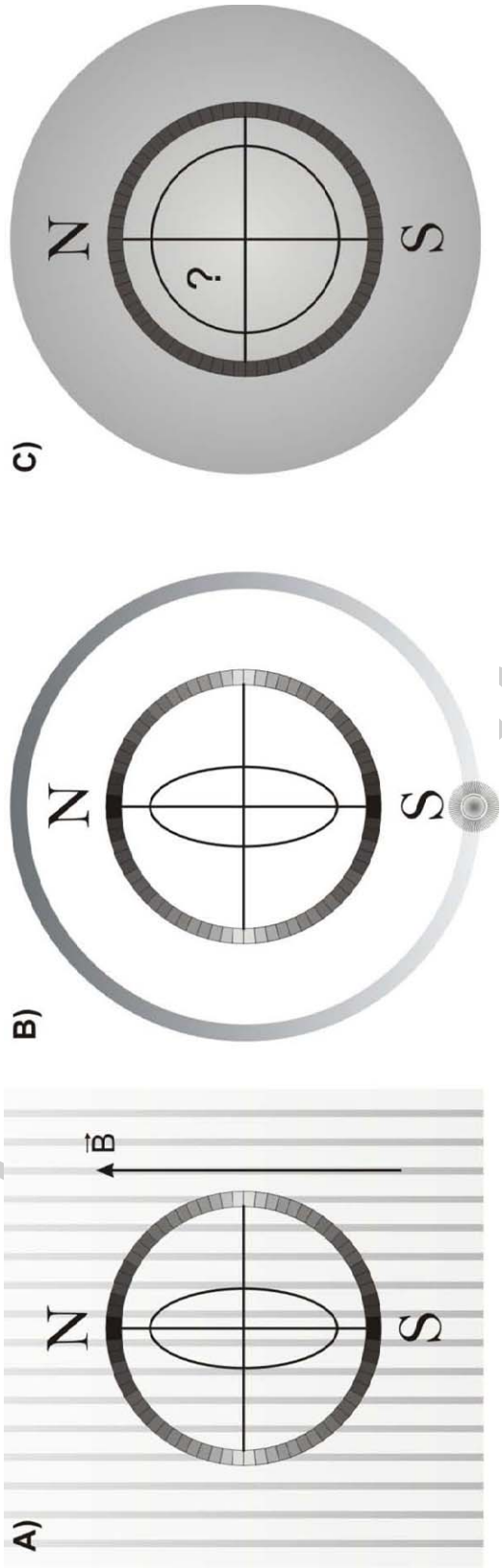

Accepted Manuscript

Figure 1

ACCEPTED MANUSCRIPT

FIGURE 2

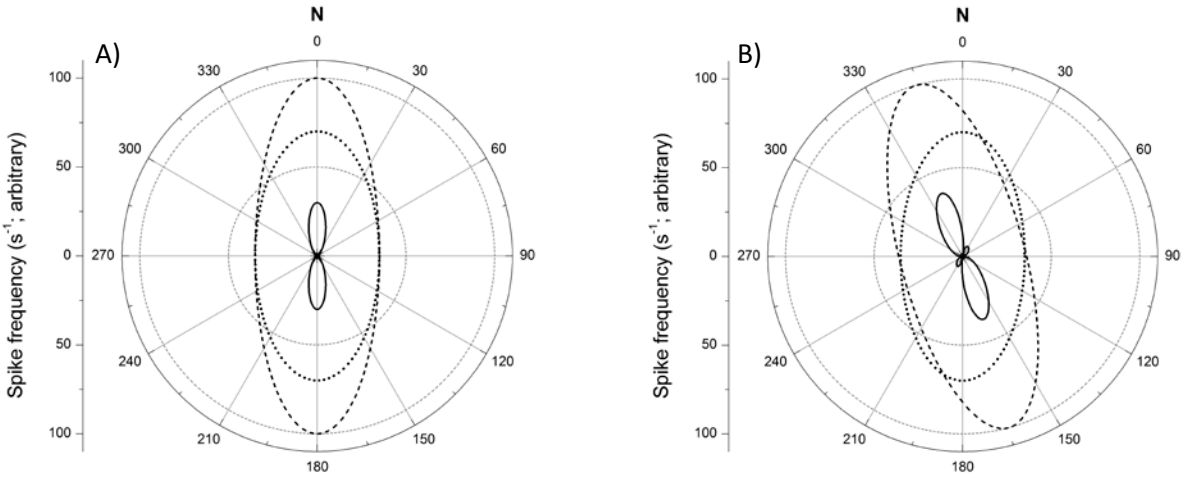

Accepted manuscript

ACCEPTED MANUSCRIPT

FIGURE 3

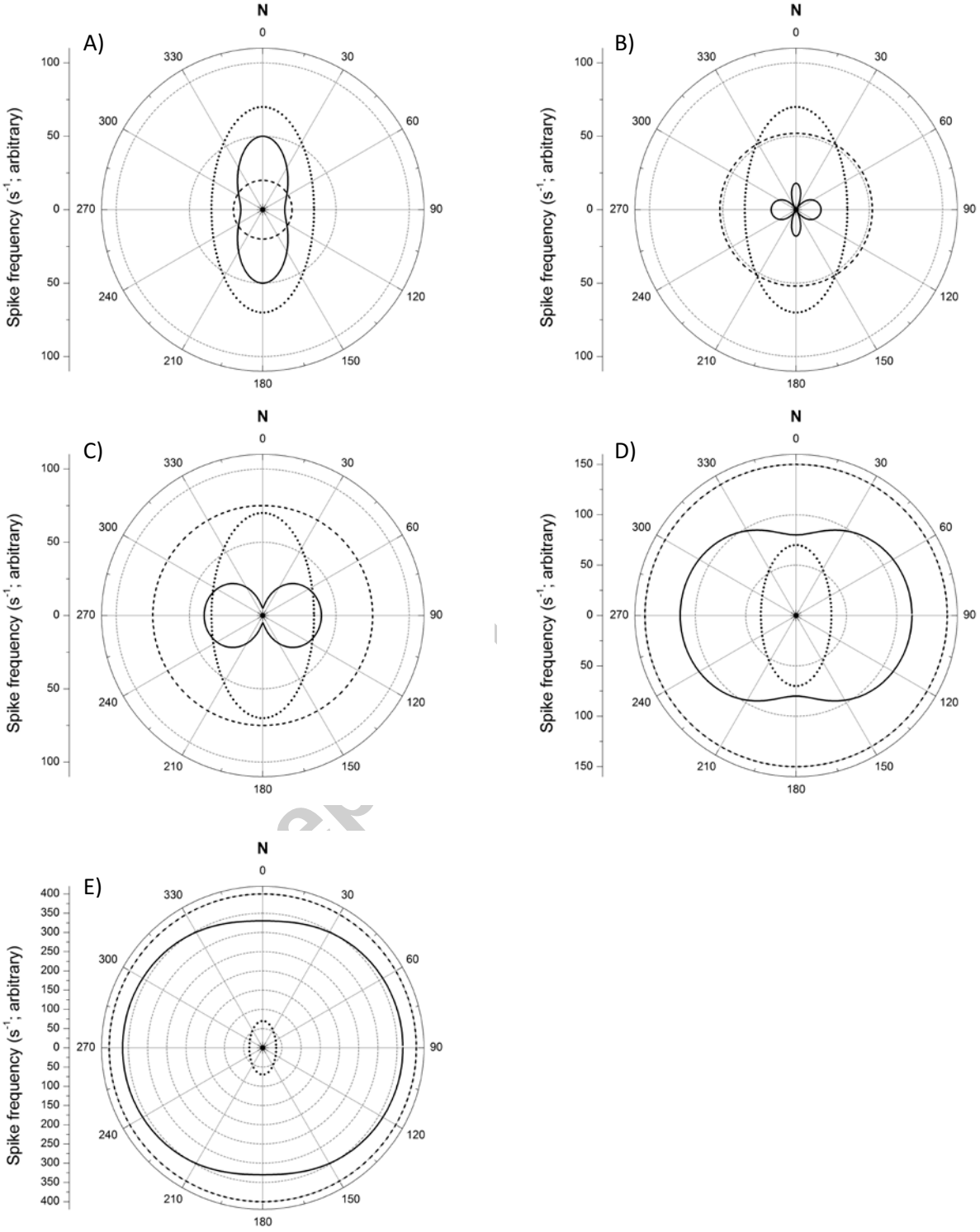

ACCEPTED MANUSCRIPT

FIGURE 4

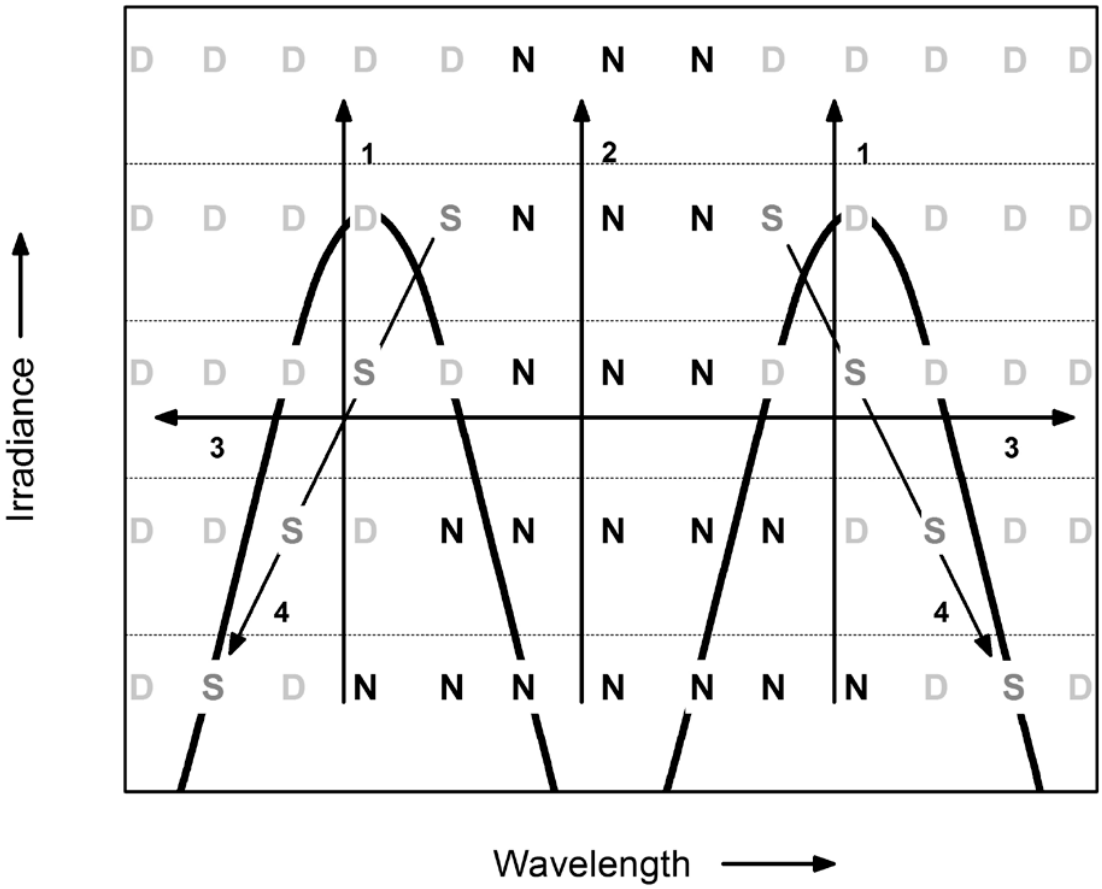

Accepte

ACCEPTED MANUSCRIPT

FIGURE 5

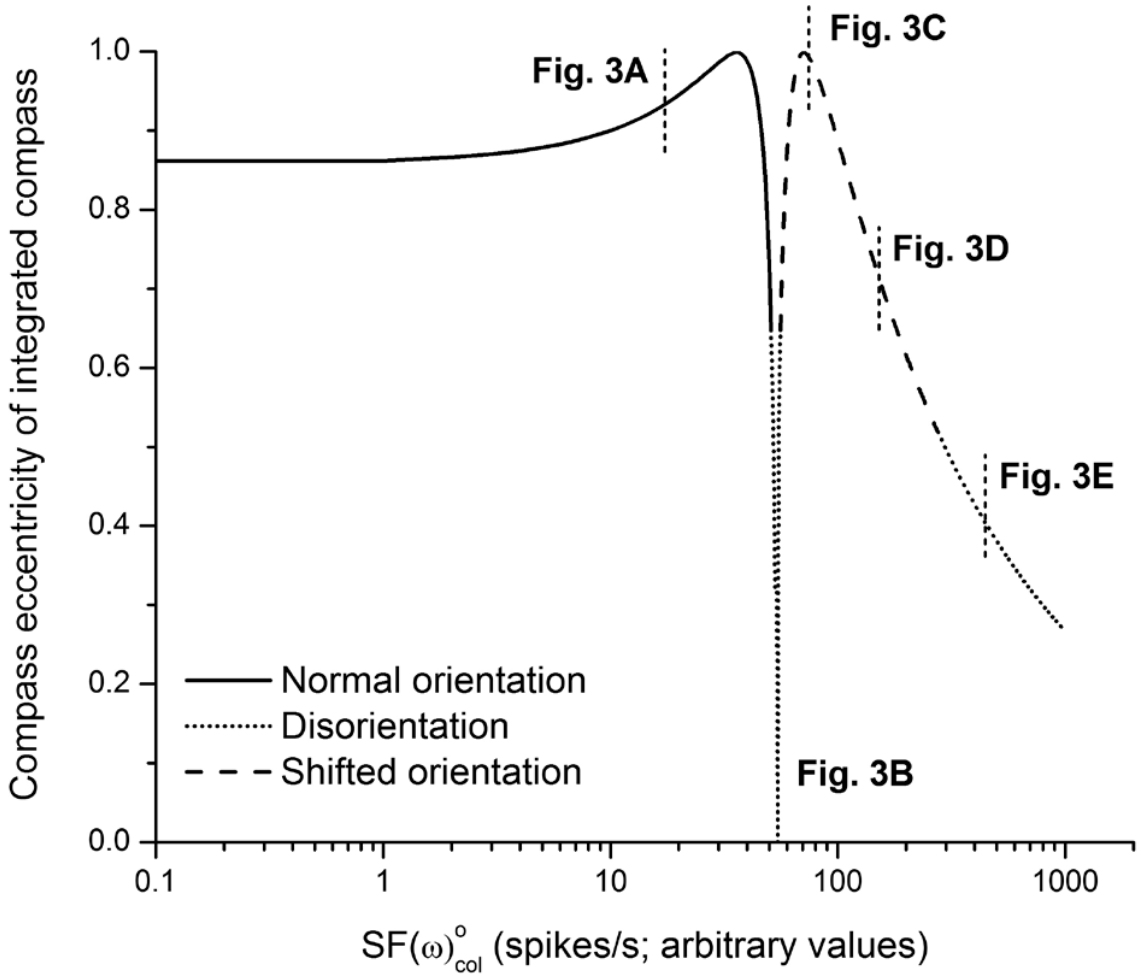

ACCEPTED MANUSCRIPT

FIGURE 6

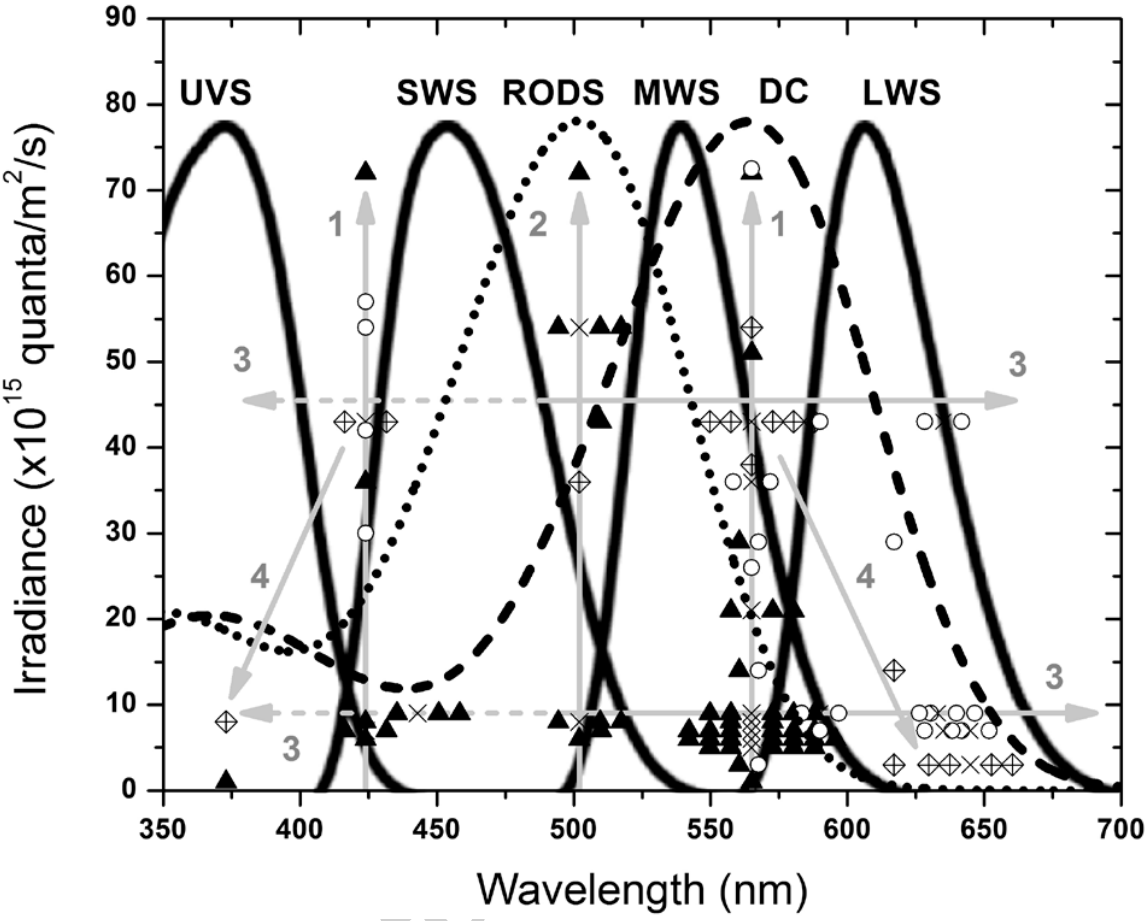

Accepted

ACCEPTED MANUSCRIPT

FIGURE 7

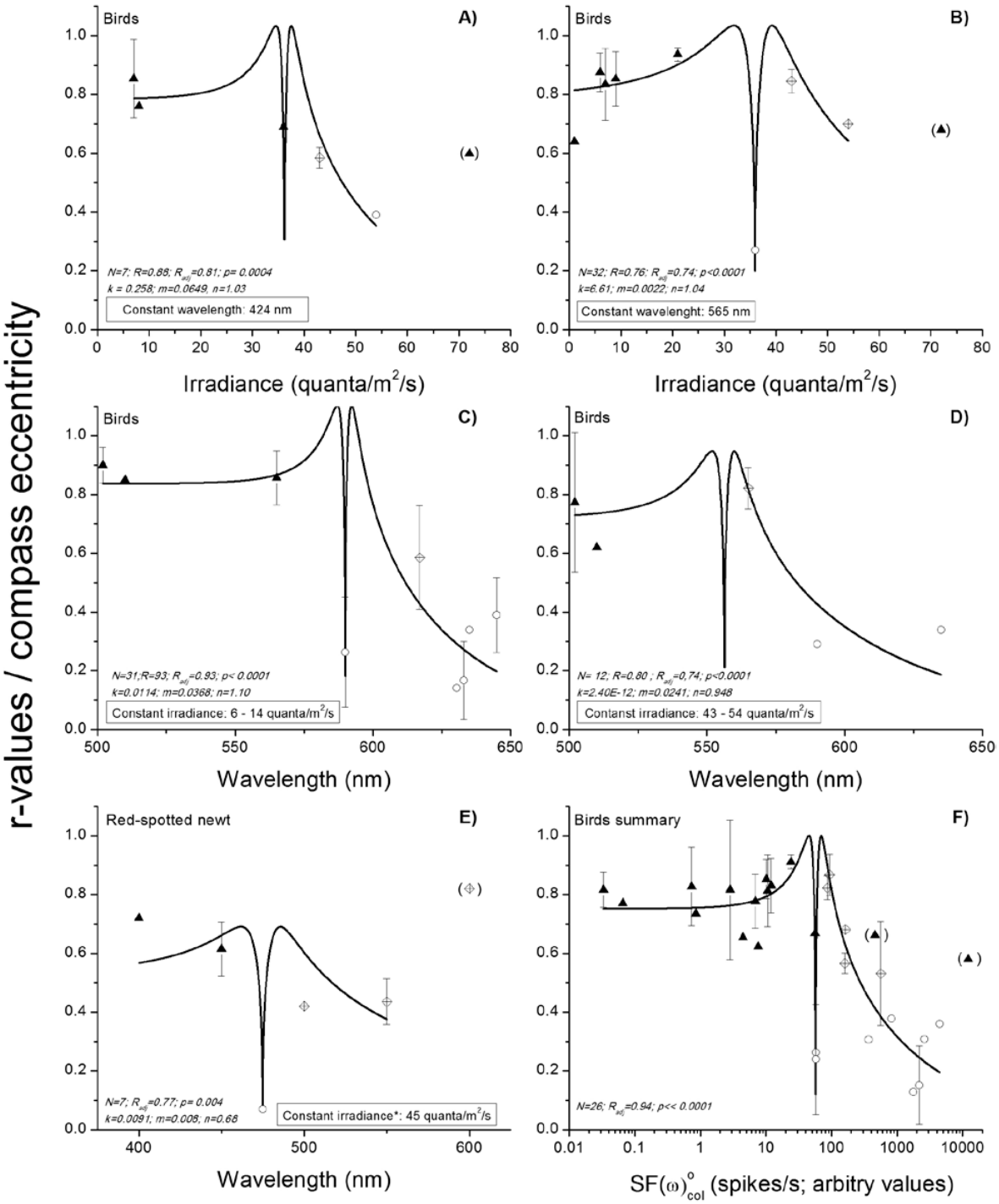

ACCEPTED MANUSCRIPT

FIGURE A1

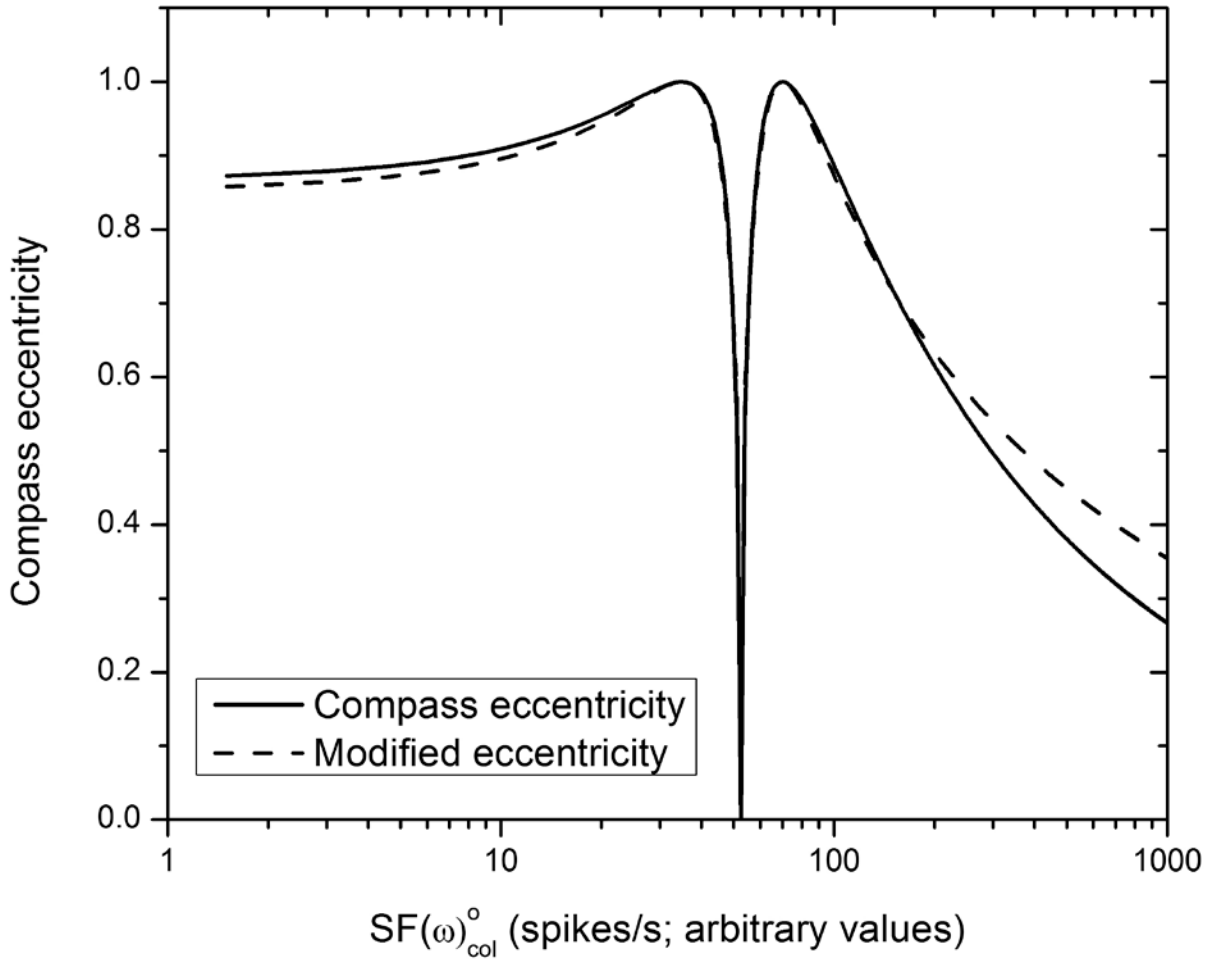

Acce

ACCEPTED MANUSCRIPT

FIGURE A2

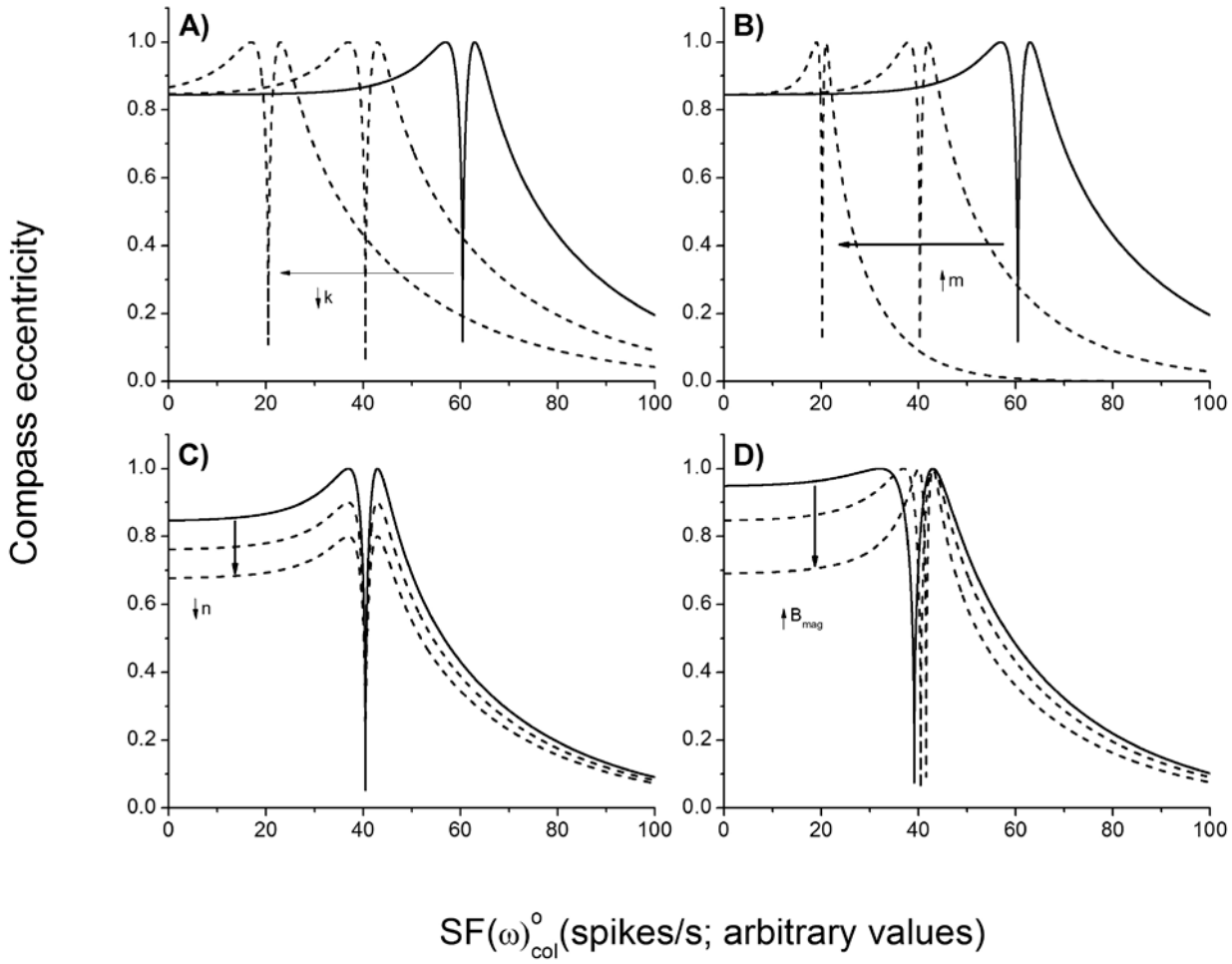

Acce

Table 1

		WAVELENGTH (nm)											
GROUP	**SPECIES**	**375**	**400**	**425**	**450**	**475**	**500**	**525**	**550**	**575**	**600**	**625**	**650**
Non-passerine birds	*Pigeon*									**N** N/A		**D** N/A	**D** N/A
	Chicken					**N** 1450							**D** 1450
Amphibians	*Red spotted newt*		**N** 22		**N** 45	**D** 45	**S** 45		**S** 45		**S** 45		
	bullfrog tadpoles						----------S---------- 13,500						
		----------N---------- 20,000											
Insects	*Fruit fly*	**N** 2					**S** 2						
	Darkling beetle	**N** 2					**S** 2						

Accepted Manuscript

ACCEPTED MANUSCRIPT

Table 2

Exp.	UV (~375 nm)	SW-MW (~500 nm)	LW (~625 nm)	COMPASS 1 *UV/LW antagonism* No reference color (Equation X)	COMPASS 2 *UV/LW antagonism* Reference color (Equation X)	COMPASS 3 *No UV/LW antagonism* Reference color (Equation X)
1a	*Constant (~20-30) ($=S_{UV.20-30}$)*	---	*Increase ($0 \rightarrow S_{LW}=S_{UV.20-30}$)*	*D → S → D → N*	*D → S → D → N*	*D*
1b	*Constant ($S_{LW}=S_{UV.20-30}$)*	---	*Increase ($S_{LW}=S_{UV.20-30} \rightarrow S_{LW}=2 \cdot S_{UV.20-30}$)*	*N→ D → S → D*	*N→ D → S → D*	*D*
2	*Constant (~20-30) ($=S_{UV.20-30}$)*	*Increase (0-80)*	*Constant low (at $S_{LW}=S_{UV.20-30}$)*	*N*	*N*	*D → S → D → N*
3	---	*Increase (0-80)*	*Constant low (~15)*	*D*	*D → S → D → N*	*D → S → D → N*
4	---	*Constant low (~15)*	*Increase (0-80)*	*N → D → S → D*	*N → D → S → D*	*N → D → S → D*

Accepted manuscript

ACCEPTED MANUSCRIPT